Evidence supporting a broader than previously thought influence of solar activity over Earth system's processes. Discussion of a possible mechanism.

Héctor Sacristán[1]

[1]Citizen scientist

Abstract:

In this article, I show lines of evidence supporting a modulation of volcanic activity and some weather phenomena by solar wind conditions in the near-Earth environment. On a daily timescale, a correlation is found between the LP earthquake activity of Kilauea volcano, related to magma transport, and the Bx component of the interplanetary magnetic field as measured in the OMNI database for specific intervals in 1995 and 2003. On yearly timescales, during the 2000-2018 period, I show a correlation between the inflation rates of four intraplate volcanoes (Kilauea, Mauna Loa, Sierra Negra, and Yellowstone) and solar wind conditions where the volcanoes' activity seemed positively correlated with solar wind dynamic pressure. Additional volcanoes also showed similar behavior to the four mentioned, in that they experienced a surge in activity in 2004-2007. I compile a list of ≥400 g hail events in Spain since 1850, from newspapers, which are given in the appendix, and is used to study the variation in the frequency of large hail events, finding a similar pattern to that seen in volcanic activity. The hail events are seen to concentrate towards the middle of the 11-year solar cycles when the interplanetary magnetic field tends to be at its strongest. Additional yearly/decadal correlations between different types of volcanic activity, Spanish hail events, and North Atlantic accumulated cyclone energy, reveal complex patterns that appear to be independent of solar activity, but show a relation between volcanism and weather processes. A possible 50-year oscillation across all three is identified. In the last section, I discuss possible mechanisms governing the observed patterns and I propose that the deformation of Earth's magnetosphere by solar wind, combined with the planet's rotation, exposes locations in the planet to a changing magnetic field which causes electromagnetic induction in ionic conductors like seawater and magma, with ensuing currents dispersing heat or having other effects, thereby influencing related processes in the atmosphere and geosphere. The possible influence of induced electric currents in magma chemistry is also discussed, after having briefly reviewed different magma compositions. I also propose 50-year oscillations to be internally driven, given there may be factors on Earth that influence the process of electromagnetic induction, but I do not try to describe any specific mechanism.

This paper is non-peer reviewed, and has not been uploaded to any journal

Contents:

1. Daily and monthly variations in the Bx component of the IMF and volcanism

1.1 Introduction

Temporal and spatial irregularities in volcanism led me to investigate and start thinking of new ideas about the inner workings of volcanic/magmatic activity. Among the complexities identified were temporal variations in volcanic activity that were seemingly widespread across the globe on various temporal timescales. Initially, I thought these were internally driven. As I did a more exhaustive inspection, however, I accidentally stumbled upon a possible relation between solar activity and volcanism in a centurial timescale, which immediately revealed a more obvious relation on a yearly timescale (the 11-year cycles in solar activity) that will be tackled in the following section (section 2) of this article. This led to suspicions that oscillations in volcanic activity were modulated externally by the Sun, leading to a reconsideration of the ideas I had been exploring, and changing the direction of the endeavor. This article will start by looking into shorter daily timescales in which solar activity and volcanism appear to be interrelated, according to the available data. My objective is to investigate the relationship between different solar activity variables and volcanic activity, to further confirm this relationship and research its nature.

1.2. Data and methods

For the variations of solar activity, I've mostly relied on the OMNI dataset (King and Papitashvili, 2005), which is an hourly-averaged, near-Earth solar wind magnetic field and plasma parameter data from several spacecrafts for the period since 1963. I've focused on the period since 1995 for which OMNI data is most complete. OMNI data were obtained from the GSFC/SPDF OMNIWeb interface at https://omniweb.gsfc.nasa.gov.

Parameters I was interested in include solar wind speed, solar wind proton density, and the magnitude and components of the interplanetary magnetic field (the magnetic field that radiates from the Sun). Of all these parameters, with limited data-analysis skills, I was only able to spot a strong link on a daily timescale between the Bx component of the interplanetary magnetic field and some volcanic activity parameters of Kilauea volcano (Hawaii, US), for specific periods. The Bx interplanetary magnetic field (IMF) component seemed to

match best the variations in volcanic activity, unlike solar wind speed and proton density. The Bx component is the intensity of the interplanetary magnetic field in the sun-Earth line. It can be positive when towards the Sun, or negative when towards the Earth according to the GSE/GSM coordinate system used.

As mentioned, I relied on the Kilauea volcano to assess the relationship between solar activity and volcanism. The reason for this is that I'm most familiar with Kilauea volcano, familiar with the way it behaves and the different parameters that could potentially be used to understand its activity. Also because earthquake data, collected by the Hawaiian Volcano Observatory, is publicly available for Kilauea, which includes the parameter I eventually chose.

During late 2023 and the first month of 2024 I followed complex episodes of volcanic unrest in the data streams provided by the Hawaiian Volcano Observatory, including earthquake swarms along the rift zones of Kilauea, and ground inflation episodes in different locations of the volcano. These crises, I observed, were correlated with periods of positive Bx IMF component, meaning periods where the interplanetary magnetic field pointed towards the sun. Periods of negative Bx component were correlated instead with relative quiescence. However, the shifting locations of unrest (between the summit of the volcano and its two upper rift zones) and difficulty in accessing tiltmeter ground deformation data made these episodes difficult to analyze or represent with simple graphs. To make graphs that represented better the link I instead looked at long-period earthquakes.

The Hawaiian Volcano Observatory earthquake location data was obtained from the IRIS earthquake browser interface at https://ds.iris.edu/ (USGS Hawaiian Volcano Observatory, 1956). Data includes a list located events which can be narrowed down by depth and coordinates to show only events originating from the LP cluster under the volcano. Long-period (LP) earthquakes originate around 10 kilometers beneath the summit of Kilauea are related to the dynamics of volcanic fluids in a conduit or crack (Matoza, Shearer, and Okubo, 2014). As such, unlike regular earthquakes, LP events are closely related to magma dynamics at the root of Kilauea's shallow magma plumbing. Unlike swarms along the rift zones, these earthquakes represent the whole volcano, because any input of magma into Kilauea's shallow system must rise beneath the summit, where these events originate. Although large swarms are only occasional, during such swarms the long-period earthquakes show large variations in terms of frequency over daily and monthly timescales, which presumably reflect changes in the activity of the volcano. Daily counts of long-period events may be a simple parameter to assess variations in magmatic activity and any possible link to solar activity.

1.3. Results

Large detected swarms of Kilauea long-period earthquakes were largely limited to the period between 1989 and 2004, which, combined with the incompleteness of the OMNI data before 1995, meant that only the 1995-2004 window was a useful period to look at correlations. The best coincidences were for 3 months in 1995, and for the second half of 2003, which will be reviewed below, in which Kilauea long-period earthquakes from the cluster 10-km deep under the summit yielded a good match with the Bx component of the IMF. There were also some weaker correlations for other swarms. Such correlations also probably exist for other parameters, like deformation or other forms of seismicity as I believe could be observed in late 2023, but which are beyond the scope of this work.

1.3.1. Kilauea 2003 LP activity

During 2003, the Bx component repeatedly changed between positive and negative values (inward and outward from the Sun) in nearly identical periods of 27.2 days. These regular changes, which have been common over the past decades, are related to the rotation of the Sun and have a mean period of 27.4 days (Xiang, Ni, and Li, 2020). Interestingly this period seems identical to the rotation of the Moon around Earth, which, coincidence or not, is rather interesting, just as a curiosity to mention.

During the year 2003, the changes in the Bx component seemingly regulated the long-period earthquake activity of Kilauea as observed in the data. Figure 1 shows the long-period earthquake daily counts versus the Bx component. During six whole 27-day solar cycles, from June to October, positive Bx enhanced LP earthquake daily counts, while a negative Bx had the opposite effect. However, in November and December, the pattern may have reversed and Kilauea experienced increased activity with a negative Bx. Related or not, this change follows the 2003 Halloween solar storms.

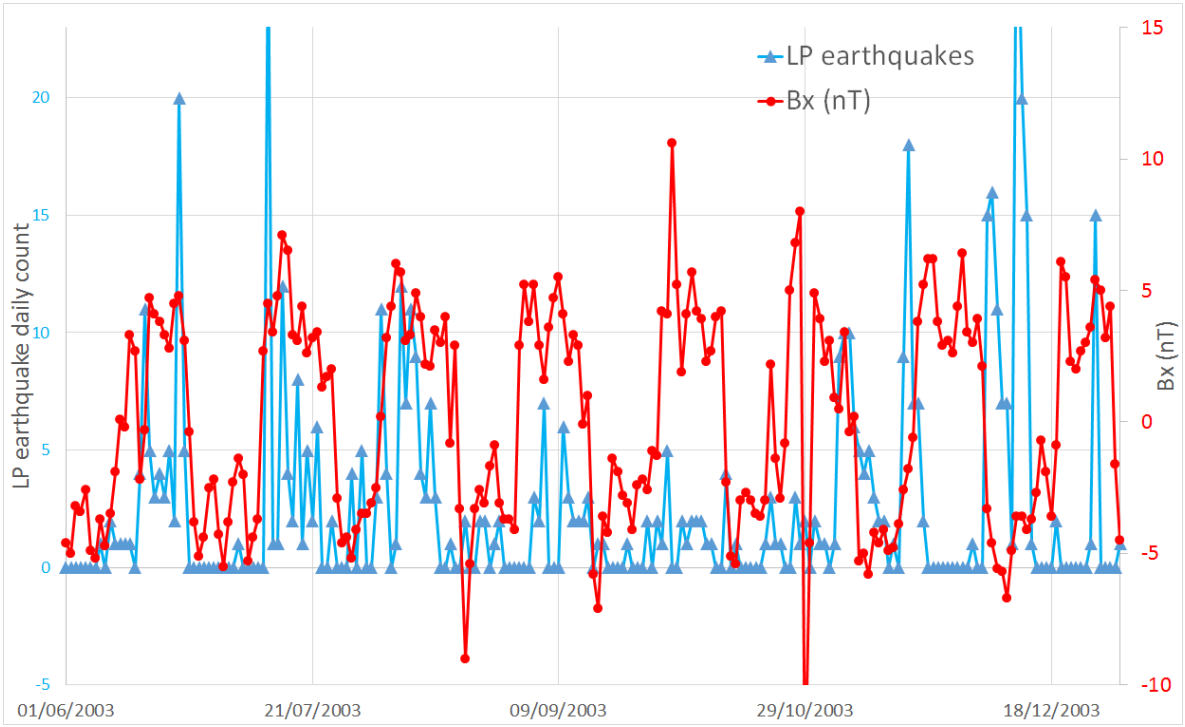

Figure 1 *- OMNI day-averaged Bx values of the interplanetary magnetic field (red circles) are compared to USGS-catalogue-based daily counts of long-period earthquakes under Kilauea (blue triangles). Horizontal axis represents time (date in dd/mm/yyyy). Data sources are described in the text (section 1.2.1).*

1.3.2. Kilauea 1995 LP activity

During 1995 the 27-day variations were less clear, and instead, there were frequent shifts in the orientation of the magnetic field at irregular intervals. Figure 2 shows the Bx and Kilauea daily long-period earthquakes for the period between 18 August and 11 November 1995, in which a strong LP swarm took place where daily counts seemed modulated by the Bx component of the IMF, presumably reflecting variations in the level of magmatic activity. In this interval, the stronger LP peaks were associated with strong negative Bx values (marked with an A in Figure 2). While some weaker peaks matched with positive Bx values. Suppressed activity coincided with intermediate Bx. In this time interval, like in 2003, there was also a correlation between the activity of Kilauea volcano and Solar activity, but this time the activity of Kilauea increased at the time of both strongly positive and negative values of the Bx in the near-Earth environment, while weaker positive or negative values suppressed activity.

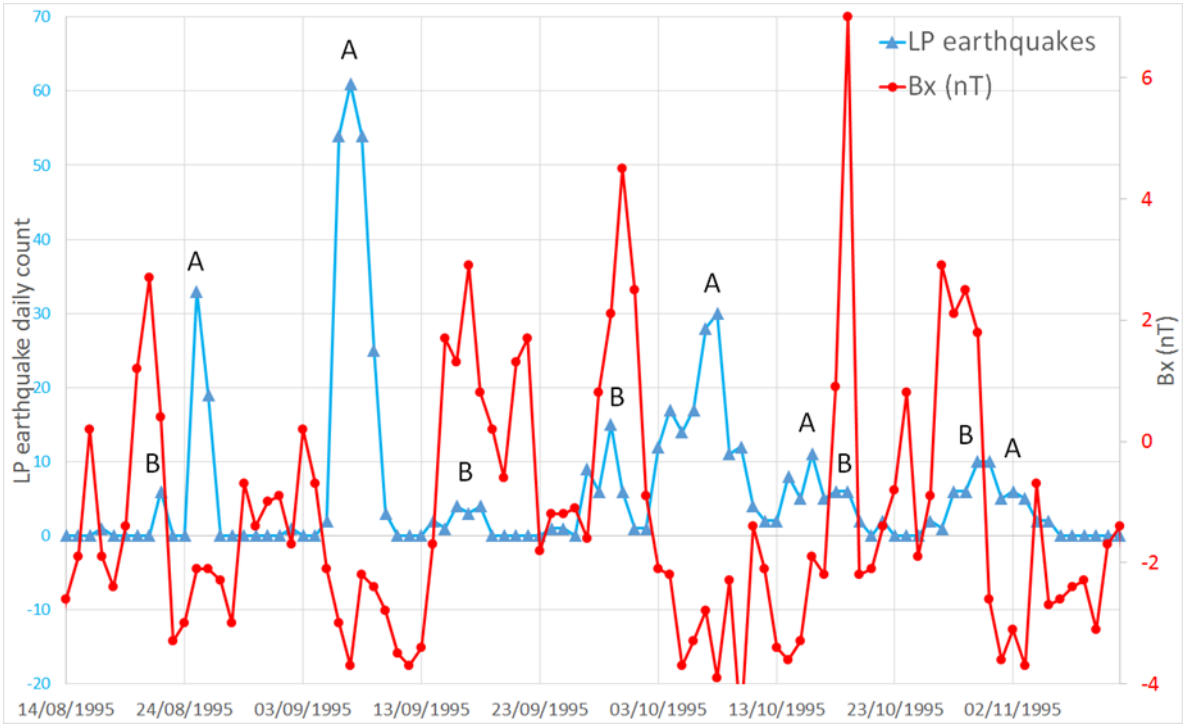

Figure 2 *- OMNI day-averaged Bx values of the interplanetary magnetic field (red circles) are compared to USGS-catalogue-based daily counts of long-period earthquakes under Kilauea (blue triangles). Horizontal axis represents time (date in dd/mm/yyyy). Data sources are described in the text (section 1.2.1). (A)-marked events are peaks in LP daily counts associated with excursions towards strongly negative Bx values, (B)-marked events are peaks in LP daily counts associated with excursions towards strongly positive Bx values.*

1.4. Conclusion

The analyzed data shows a correlation between the Bx component of the IMF and the volcanic activity of Kilauea volcano. Since LP earthquakes are linked to magma transport, this can be interpreted as a correlation between solar activity and ensuing space weather with magma transport on Earth. It would be much easier for solar activity to influence Earth's processes given that space weather extends into our planet's environment and is already known to trigger other well-known effects such as auroras or damage to power grids. As such it may most likely be viewed as a modulation of volcanism by solar activity. Although I believe this data is already enough to show a solid connection, extraordinary claims require extraordinary evidence, so I will present further data for other timescales as well as similar relationships seen in weather. It also seems worth looking for more cases of daily correlations in volcanic and solar activity by examining seismic data or surface activity observations at other volcanoes, ideally for various parameters, tectonic settings, and geographic areas, which is however beyond the scope of this work.

2. Yearly variations in solar activity and volcanism

2.1. Introduction and observations

I observed, while reviewing volcanic data of the past decades, that global pulses of volcanic activity took place during specific years, only later did I notice these pulses seemed to repeat following sunspot solar maximums of the 11-year solar cycles. It turned what I thought to be internal phenomena into external influence. Most notably there was a volcanic pulse during approximately 2004-2007, that seemed to affect many important intraplate volcanic regions, followed by a smaller pulse around 2015. Both pulses happened in the years following the 11-year sunspot peak. What follows is a compilation of some of the most noteworthy cases of heightened activity during the 2004-2007 pulse, which seems the stronger one of the two. Among the examples are four ocean island provinces, which are some of the most productive on the planet (Hawaii,

Galapagos, Reunion, and Comoros), as well as Yellowstone (US), the largest volcanic caldera in the world. There might be multiple subduction zone volcanoes too, though from among them I'm only looking at Manam:

-Hawaii (US): Kilauea, the most active volcano in Hawaii, and arguably the most active volcano in the world in terms of overall lava production, had a major, well-described magma surge in 2003-2007 where the magma supply into the volcano at least doubled (Poland et al., 2012). Carbon dioxide emissions and inflation rates, both representative of supply, peaked in 2005 and 2006 respectively. As we will see in section 2.3, Mauna Loa, the largest and second-most active volcano in Hawaii, had a major magma supply pulse peaking in 2005. This Mauna Loa surge was also associated with the volcano's largest recorded swarm of long-period earthquakes, which took place in 2004-2005 (Okubo and Wolfe, 2008).

-Galapagos (Ecuador): Fernandina, the most frequently erupting volcano in the Galapagos Islands had a small activity surge in 2005-2009, which includes an eruption in 2005, followed by sheet intrusions under the southeast flank in 2006 and 2007, and a final eruption in 2009 (Bagnardi and Amelung, 2012).

Sheet intrusions are events where magma pours into growing cracks within the rock, that may or may not intersect the surface producing an eruption. Eventually, sheet intrusions solidify into blades of magmatic rock. They work similarly to eruptions in that they remove a volume of magma that has built up within the storage of the volcano, draining the storage that needs to be refilled before another event. As such, the frequency of both intrusions and eruptions in shield volcanoes roughly approximates the supply rate. The cluster of intrusions and eruptions of Fernandina in 2005-2007 indeed coincides with rapid inflation rates of the volcano (Bagnardi and Amelung, 2012) so must represent a particularly high supply.

In section 2.3, I will look at Sierra Negra ground deformation, the largest Galapagos volcano, which also experienced a magma surge at this time, peaking in 2006, and associated with a 2005 eruption.

-Reunion (Overseas France): Lava production in the Reunion volcanic province is historically entirely represented by Piton de la Fournaise volcano, arguably the most frequently erupting volcano on the planet, which often produces multiple fissure eruptions per year, but can also be dormant for a few years. Piton de la Fournaise had a period of exceptional productivity in 2004-2007 (Vlastélic et al., 2018, and references therein), even without considering the climactic eruption of April 2007. This high productivity came in the form of some unusually voluminous long-lived eruptions that took place in 2004, 2005, and 2006. Gradual pressure build-up led to a climactic eruption in April 2007 that emptied and collapsed summit storage and was the largest eruption of the volcano in over a century. After a series of small eruptions in 2008-2010, there was a long dormancy until 2014, followed by a resumption of high lava production rates starting in 2015.

-Comoros: All historical subaerial eruptions of the Comoros Islands have originated from Karthala volcano. After an extended 14-year dormancy, Karthala volcano erupted four times between 2005 and 2007 (Global Volcanism Program, 2024b), which represents the only activity of the volcano in the 21st century, and one of the most intense activity episodes of the volcano historically.

-Yellowstone (US): Yellowstone volcano experienced a magma surge in 2005-2008 (see below) which involved uplift of the entire caldera. A quiescent period characterized by deflation followed until another uplift episode in 2014-2015.

-Manam (Papua New Guinea): Unlike Hawaii, Galapagos, Reunion, Comoros, and Yellowstone, which are intraplate volcanoes, Manam is a subduction zone volcano located in a tectonic plate boundary. It's a very active volcano. Manam experienced a series of 7 or more paroxysmal explosive eruptions between 2004 and 2006, most of them in 2004 (Global Volcanism Program, 2024c). The 2004-2006 eruptions are considered the most destructive series of recorded eruptions at Manam, with ash reaching heights of possibly up to 24 kilometers into the atmosphere. The volcano did not produce another large paroxysmal eruption until 2015.

There are probably other subduction zone volcanoes apart from Manam that also reflect the 2004-2007 pulse, like Saint Helens or Lopevi. But it's harder to get a good grasp of how magma supply has evolved in such volcanoes since it depends on the type of volcanic activity displayed. Subduction zone volcanoes often erupt

without producing much lava volume, displaying only low-level explosive activity. Actual periods of high lava production involve effusion of lava flows and explosive paroxysms, but information regarding whether these modes of activity are present or not, or the exact timing, is often difficult to compile.

Since there is a worldwide pulse in, at least intraplate, volcanic activity during 2004-2007, there is the question of what caused it. A smaller follow-up surge took place in 2015 in many of the volcanoes previously mentioned. The pattern seemed to align with the 11-year cycles of solar activity, with volcanic activity spiking in the phase of decreasing solar activity after the solar maximum, later I saw that in the near-Earth environment, solar wind conditions peak about 2 years after the sunspot maximum. For example, as recorded in NASA's OMNI database, all, solar wind dynamic pressure (plasma flow), absolute value of the Bx component, and IMF magnitude, peak in 2003 and 2015 (see below) for their respective 11-year solar cycles, matching both aforementioned surges. My next objective will be to illustrate this match.

2.2. Data and methods

To gauge magma supply a simple way is to look at volcanic deformation. As magma rises into a volcano, the volume of its magma storage expands and displaces the surrounding rock, which results in uplift. The uplift rate should be roughly proportional to the magma supply. That's why I've looked at the uplift rate of GPS stations of four volcanoes, the data is distributed by the Nevada Geodetic Laboratory (Blewwit, Hammond, and Kreemer, 2018). The stations used are AHUP for Hawaii's Kilauea volcano (Segall and Miklius, 1999), MOKP for Hawaii's Mauna Loa volcano (Miklius, 2000), WLWY for North America's Yellowstone caldera (UNAVCO community and Smith, 2001); and GV01 for Galapagos' Sierra Negra volcano (LaFemina et al., 2012). The data dates back to around 2000 in most volcanoes. Volcanic deformation data earlier than 2000 is too scarce for analysis. I also interrupted analysis in 2018 due to significant specific circumstances of Kilauea and Sierra Negra that led to changes in deformation, these being the effusion cessation and collapse of Kilauea in 2018 and the very voluminous eruption of Sierra Negra in the same year (Global Volcanism Program, 2024a).

I've compared the GPS data to solar wind parameters from the OMNI dataset (King and Papitashvili, 2005). Solar wind parameters can probably be divided into those regarding the magnetic field, the IMF magnitude and its three components, and the mechanical aspect, which is the solar wind synamic pressure derived from plasma density and wind speed. Both groups vary roughly similarly throughout the period, but I found the match of uplift rates with solar wind synamic pressure to be somewhat better. As such, I will use solar wind dynamic pressure in the graphs shown in the following section. That said, I do not mean to show which specific solar wind parameters are more closely related to volcanism, but rather to show that there is a general link between solar wind conditions and volcanism.

2.3. Results

As seen in figures 3 to 6, uplift rates of each Kilauea, Mauna Loa, Sierra Negra, and Yellowstone reflect a common pattern. Starting from low activity, all four volcanoes rise to a peak in magma supply in 2005 or 2006. All except Kilauea dropped to a low in activity around 2010-2012. Kilauea has an earlier drop, but this is likely related to internal dynamics, due to the opening of a lower elevation volcanic vent, the TEB vent (Orr, Llewellin, and Patrick, 2022) that led to early deflation of the volcano due to increased eruption rates, keeping in mind that Kilauea was continuously effusing lava during this period until the 2018 eruption. Sierra Negra rose to a second peak in 2013, Yellowstone and Mauna Loa peaked in 2014, and Kilauea in 2015. All but Yellowstone show a relatively high supply in the years after 2015.

As such, something is modulating the activity of different volcanoes throughout the world. Figures 3 to 6 compare uplift rates with solar wind dynamic pressure (a derived parameter of plasma density, and solar wind speed), showing a relatively good match between both parameters and suggesting the causal mechanism lies, at least partly, in solar activity.

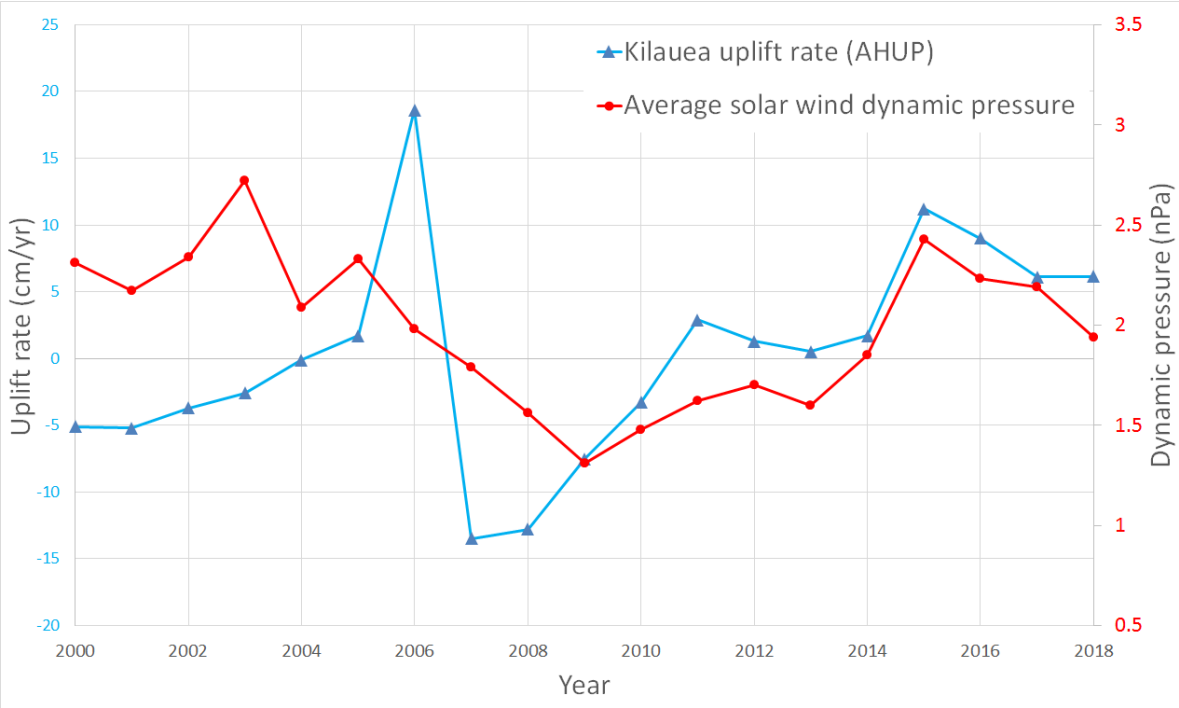

Figure 3 *– The uplift rate of AHUP GPS station in the south caldera area of Kilauea (Hawaii) is compared to solar wind dynamic pressure over the same period. 2007 saw the opening of the TEB vent. The data source is described in the text (section 2.2).*

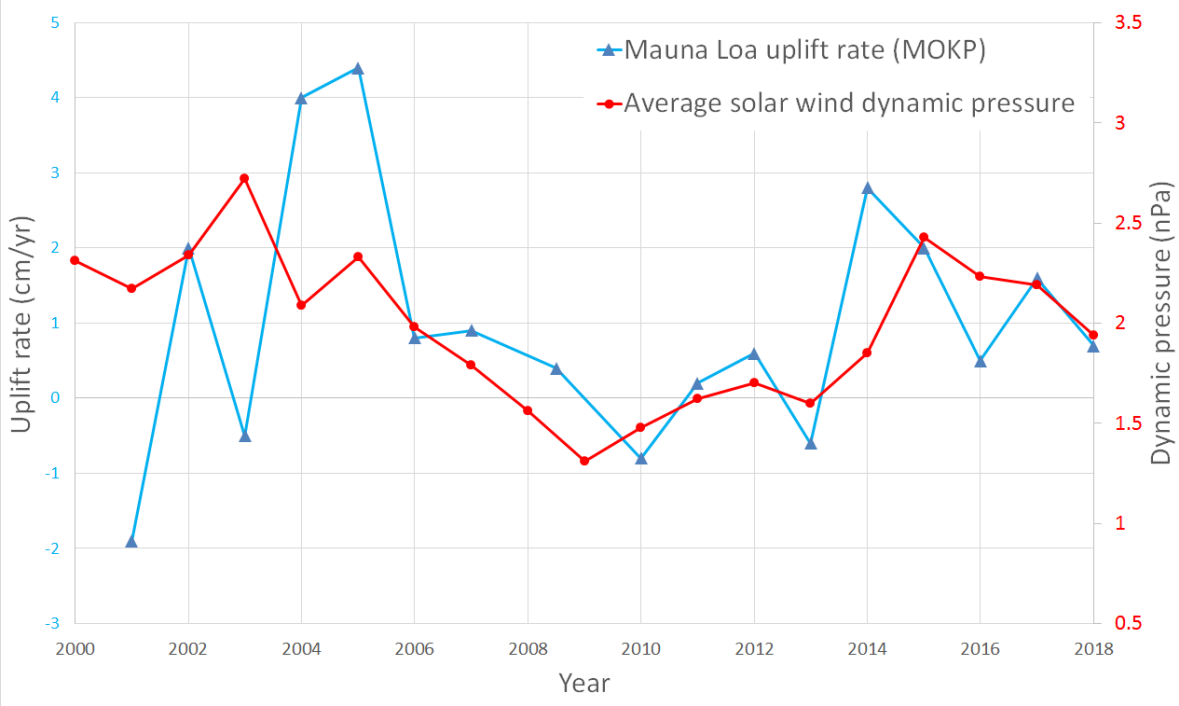

Figure 4 *– The uplift rate of MOKP GPS station on the caldera rim of Mauna Loa (Hawaii) is compared to solar wind dynamic pressure over the same period. Data source is described in the text (section 2.2).*

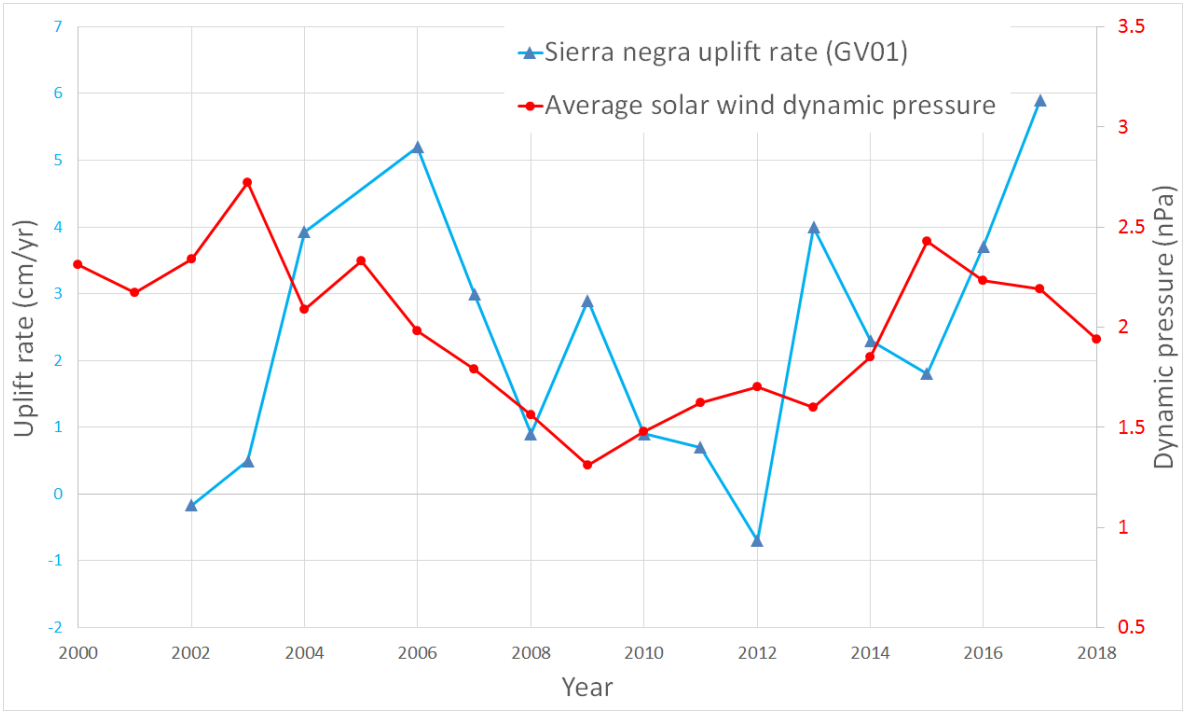

Figure 5 *– The uplift rate of GV01 GPS station on the caldera rim of Sierra Negra (Galapagos) is compared to solar wind dynamic pressure over the same period. 2005 eruption deflation is excluded from graph since is unrelated to supply variation. Data source is described in text (section 2.2).*

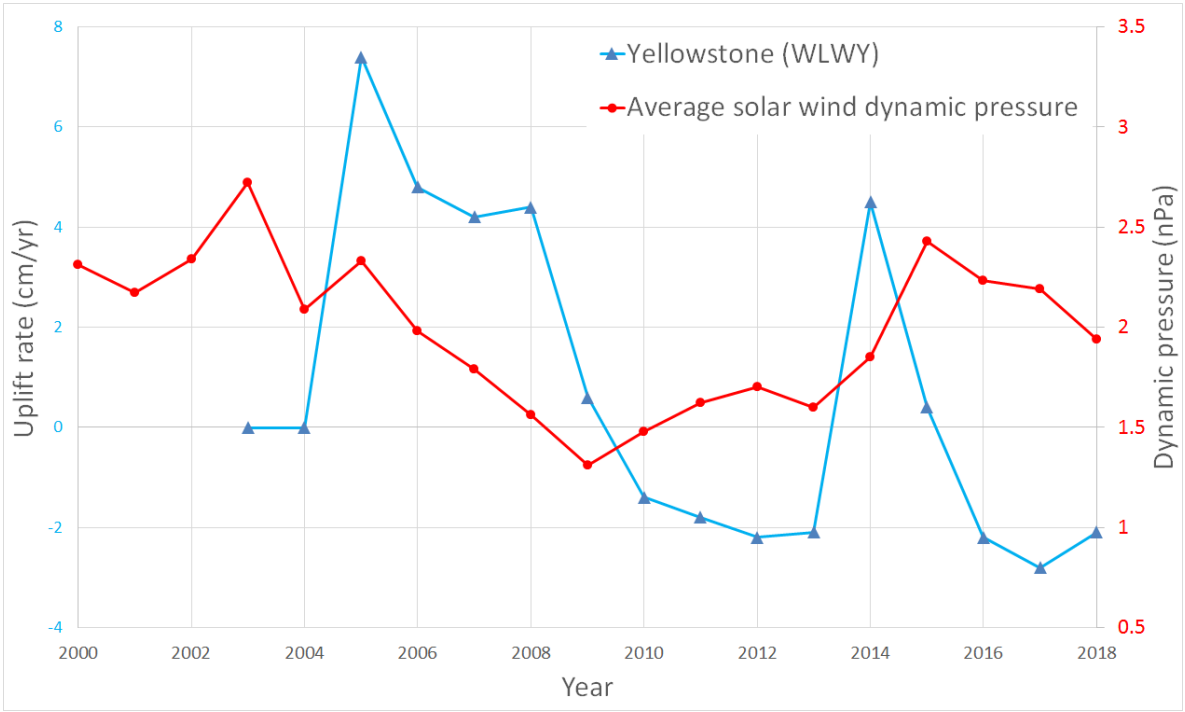

Figure 6 *- Uplift rate of WLWY GPS station within the caldera of Yellowstone (US) is compared to solar wind dynamic pressure over the same timespan. Data source is described in the text (section 2.2).*

2.4. Discussion and conclusions

Volcanic activity in many different volcanoes of the world shows a similar evolution of supply over time. Many important volcanoes experienced a major magma surge around 2004-2007, followed by a reduction in activity before activity increased again from 2013 onwards. A magma surge likely implies an increase in the rate of magma generation within the planet. An increase in magma generation may imply higher temperatures that bring rock closer to its melting point and accelerate existing mechanisms of magma formation in tectonic plate boundaries and intraplate areas. There's even the possibility that solar wind is itself the dominant mechanism of magma generation in certain intraplate areas. A possible explanation is that there is a mechanism for solar wind to transfer energy into our planet's interior and that changes in solar wind dynamic pressure or other space weather conditions influence magma production. Though as seen in section 6 Earth may also influece this energy transfer from its own end. It may be important to consider that volcanism is a surface reflection of larger scale magmatic processes within the Earth.

3. 11-year cycles and hailstorms

3.1. Introduction and observations

Solar cycles are quasi-periodic variations in solar activity where solar flares and sunspot number and size rise from a minimum to a maximum and go back to a minimum. During each solar cycle, the magnetic field of the Sun flips. They last approximately 11 years. During these cycles, solar wind parameters such as the magnitude of the magnetic field or the speed of the solar wind also experience cyclic variations. I have already discussed the relation with volcanism and some of the last solar cycles, in this section, I will discuss the relation to a specific weather phenomenon.

A series of large tornadoes took place in the same geographic area of Spain, the Teruel province, in 1999, 2003, and 2004. These three tornadoes tracked for lengths of 8-14 kilometers, reached widths of a few hundred meters and caused severe tree damage along their path (Conesa, 2006). I found it enigmatic that no further tornadoes of comparable size had affected the Teruel Province since. This geographic area is particularly prone to large supercell thunderstorms within Spain, which are known for spawning mesocyclonic tornadoes and giant hail, but apparently, they were particularly capable of doing so in those few years, and not quite as much since. One of the things that occurred to me is that it had to do with solar activity, since solar cycle 24, the one that included these tornadoes, was much stronger in terms of sunspot number than the two subsequent cycles. Regardless of whether this was correct or not, it compelled me to investigate Spanish newspapers for old tornado and giant hail events that could be compared to solar activity.

3.2. Data and methods

My objective was to compare Spanish supercell-related weather to volcanism or solar cycles. Since 11-year solar cycles experience cyclic variations in solar wind parameters I speculated there would also be cyclic variations in weather patterns related to such solar cycles even for former times where OMNI data is not available. The problem is that not all solar cycles last the same time or have the same shape. The start and end of solar cycles in the analysis are as traditionally given by the Royal Observatory of Belgium (SILSO sunspot data), which correspond to the month with the lowest sunspot number. I have assigned weather events to the eleventh fraction of the solar cycle in which they take place. For commodity and intuitiveness, I will refer to this as year of the cycle, since solar cycles have an average 11.1-year duration. For example, year 0 of the cycle is the first eleventh fraction of each solar cycle, year 1 is the second eleventh, and so on. That way I account for the different durations of solar cycles, although not their "shape".

I've again relied on the OMNI dataset. I have compared solar wind parameters to their position within the cycle to understand how solar wind parameters change during a typical solar cycle. In general, most of them, like proton density, the solar wind dynamic pressure, the magnitude of the interplanetary magnetic field, and the Bx component of this magnetic field, all peak during year 6, or sometimes 5 of the solar cycle, contrasting with solar sunspot number which instead tends to peak during year 4. It could be due to the known shift in solar activity towards lower latitudes of the Sun later in the cycle, affecting Earth more directly after the actual sunspot maximum (Ivanov, Miletskii, and Nagovitsyn, 2011). Regarding the Bx component, I've used the absolute value of this component to consider both negative and positive Bx as a parameter that may affect weather, similar to how Kilauea activity seems to be enhanced by both strongly negative and strongly positive Bx values (figure 2). OMNI data includes solar cycles 20-24, so I use them to analyze how the different parameters evolve, excluding solar cycle 25 which is unfinished.

I searched for hailstorms and tornadoes in Spanish newspapers. Tornadoes were difficult to identify in newspapers, often being unclear if the event was a tornado or some other severe wind event. There were also few straightforward tornado reports to be found. Instead, hail was surprisingly well documented in newspapers to the point that many thousands of large hail events are probably documented in Spanish newspapers. For many events, the weight of hailstones and damage is described. There was also a surprisingly large number of very heavy hailstones found in this literature, as well as a very high number of damaging hail events in major cities. For example, I found mentions of 6 hailstorms that broke windows in the center of Madrid (Spain's capital) in 1889-1904, where at least 5 of them reached chestnut/pigeon egg size or greater. These 6 hail events took place in only 15 years. At present, as far as I've found, the center of Madrid has only been grazed by a 2008 event of such magnitude, and before that it hadn't seen one since 1949.

Due to the usefulness of hail reports, I will rely on these for the analysis. At present, 658 hail events with reported stone weight have been compiled, as well as a total of 2176 large hail events with some level of size information and within present-day Spanish territory, although there are still some newspapers and keyword searches to be included. I think however that ≥400 g hail since 1850 will suffice for the analysis of this article so that a full list of the hail events employed can be given in the appendix, a total of 118. The method I will use is simply to compare the number of recorded events to year of the solar cycle (eleventh of the cycle). I will also use this data again in later sections. Each event is one hailstorm. If there are different weight reports for a storm it still counts as one.

The weight reports seem reliable to me for several reasons. One is that many reports are very detailed, even for the largest values that would be hard to believe otherwise. For example, the 17 August 1952 hailstorm in Baleares had two independent reports of 1.5 kg hailstones. In one of them, it's specified the hailstone opened a whole so large as to allow a man through in the roof of Es Llombars church, then collected and measured in 1.5 kg. The other report refers to Campos district and comes from a conversation of first-hand witnesses within this district to the author of the report, the witnesses having weighed "for curiosity" some hailstones that exceeded 1.5 kg. Another example is the 11 September 1949 Cartagena storm where two witnesses of a hailstone being measured at 1.5 kg talked to the local Cartagena newspaper that later issued this information. And also in the 16 August 1948 Tudela hailstorm, the quote of a school director, claiming to have weighed a 1.5 kg hailstone himself, is given in the newspaper. These events are described in the appendix to the article.

Particularly large hailstones are also clustered in specific years which generally correlate with high hurricane activity over the Atlantic (section 4.3.2). There's most notably the 1947-1952 cluster with 17 reported events that have hailstones exceeding 400 g in weight, whereas there are longer periods with no such reports. 1915 has five 400 g+ hail reports, most of them extensively described, yet the 11 years from 1916 to 1927 have only two such events. 1915 has a total of 15 reported large hail events with some degree of information, while 1919 and 1920 have 20 and 24 respectively yet no ≥400 g hail whatsoever. This argues against such reports being mistakes or exaggerations, since, if this was the case, distribution would be random and correlate with years of overall higher large hail incidence. Instead, ≥400 g events correlating with specific years or storm outbreaks makes me confident in the reliability of the weight data as it's expected that specific intervals will have weather conditions favorable for particularly extreme hail to exist, and in the case of data being wrong these would not show. Regarding specific outbreaks, for example, out of seven storm outbreaks with ≥400 g reports for the well covered by newspapers Guadalajara-Madrid-Toledo-Ciudad Real provinces since 1870, six of them have multiple independent reports of hailstones reaching similar weight values within the same 1-3 day interval. Similar examples also exist for lower weight values in this same region.

Other spatiotemporal patterns can be seen. Such as ≥750 g hail being almost absent from 21 July to 16 August, yet having remarkably high frequency from 16 August to 14 September, across the whole country and all the period covered. ≥600 g hail is also entirely limited to the eastern side that has Mediterranean wind influence since 1850, save one case, despite large hail being destructive and commonly reported for the northwestern quarter of the Iberian peninsula, where reports do not seem to go above 500 g however. All of the aforementioned reasons make me confident in the reliability of hail weight data in historic news sources.

3.3. Results

Table 1 sums up hail data during solar cycles 10, 12-16, and 18-21, selected to avoid wars in which data is lacking or incomplete. Figure 7 plots the number of ≥400 g hail together with solar wind dynamic pressure versus the year of the cycle.

≥400 g hail activity in Spain shows a peak towards the middle of the solar cycle for the cycles considered, peaking in years 4-6 of the cycle for both median and average counts of ≥400 g hail. When compared to OMNI solar wind parameters, hail shows a better match with the IMF magnitude than with the solar wind dynamic pressure. On average, solar sunspot maximum occurs during year 4 of the cycle, so both hail and IMF magnitude peak ~1-2 years after the traditional maximum, showing a positive correlation. Although, regarding effects on Earth, the peak should be that of the IMF magnitude and solar wind dynamic pressure, about 1-2 years after the sunspot maximum.

Although the number of events used here is limited, I'm working in the larger dataset mentioned earlier, and preliminary results also indicate a well-defined peak in hail activity centered on year 6 of the solar cycle for larger numbers of smaller events too.

News-reported ≥400 g hail in Spain during solar cycles 10, 12 to 16, and 18 to 21 (excluding those including the Third Carlist War and Civil War)

Year in the cycle	SC 10	SC 12	SC 13	SC 14	SC 15	SC 16	SC 18	SC 19	SC 20	SC 21	Average	Median
0	0	0	3	1	2	0	1	0	0	1	0.8	0.5
1	1	0	0	0	0	1	1	1	0	0	0.4	0
2	0	3	0	2	5	0	0	0	0	0	1	0
3	4	0	3	0	0	0	2	0	0	0	0.9	0
4	1	0	2	1	0	2	4	1	0	0	1.1	1
5	1	5	2	2	0	1	2	1	0	0	1.4	1
6	1	4	1	1	0	1	6	1	0	2	1.7	1
7	1	0	2	0	0	0	0	0	0	0	0.3	0
8	3	0	0	1	1	0	0	2	0	1	0.8	0.5
9	0	0	2	1	0	1	3	0	1	0	0.8	0.5
10	0	0	2	1	0	0	0	0	1	1	0.5	0
Total	12	12	17	10	8	6	19	6	2	5	9.7	4.5

Table 1 *- Year of the cycle refers to the eleventh of each solar cycle. The columns in green background show 400 g+ hail event counts for year of the cycles. It includes cycles 10, 12-16, and 18-21 leaving out two wars that seem to have reduced or interrupted data. Cycles 22-24 have none or too few events to include them.*

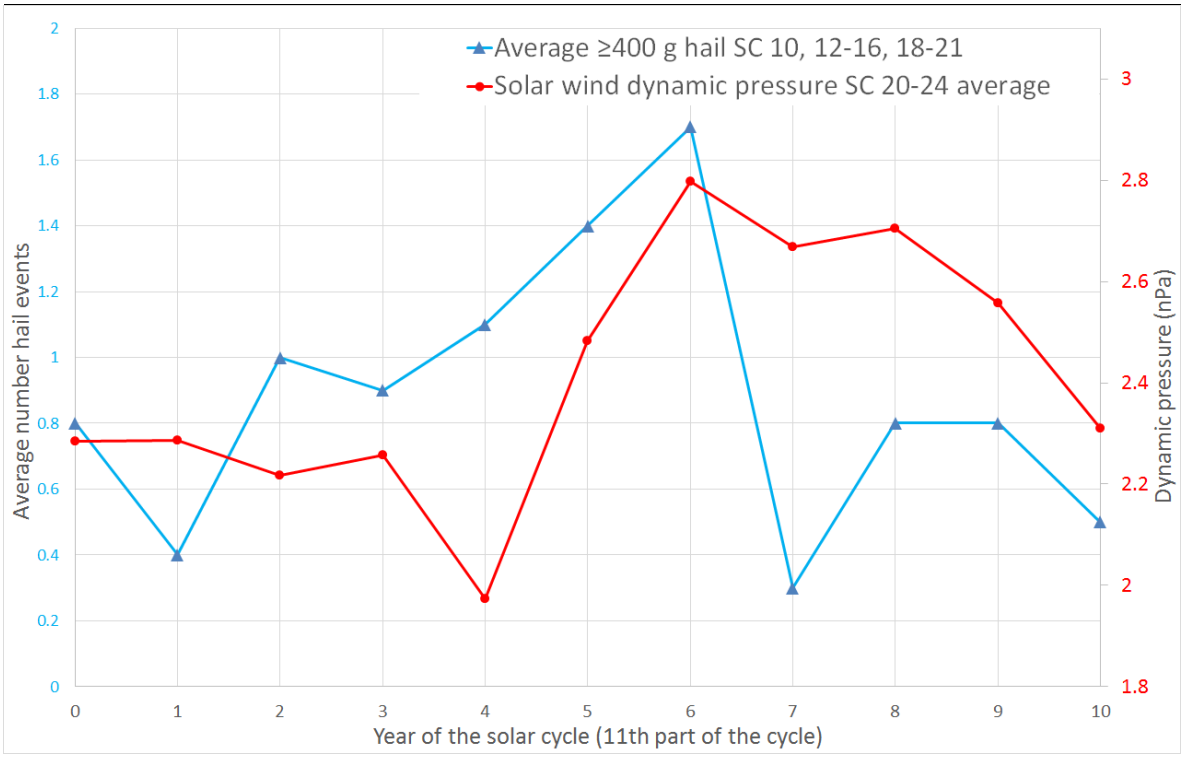

Figure 7

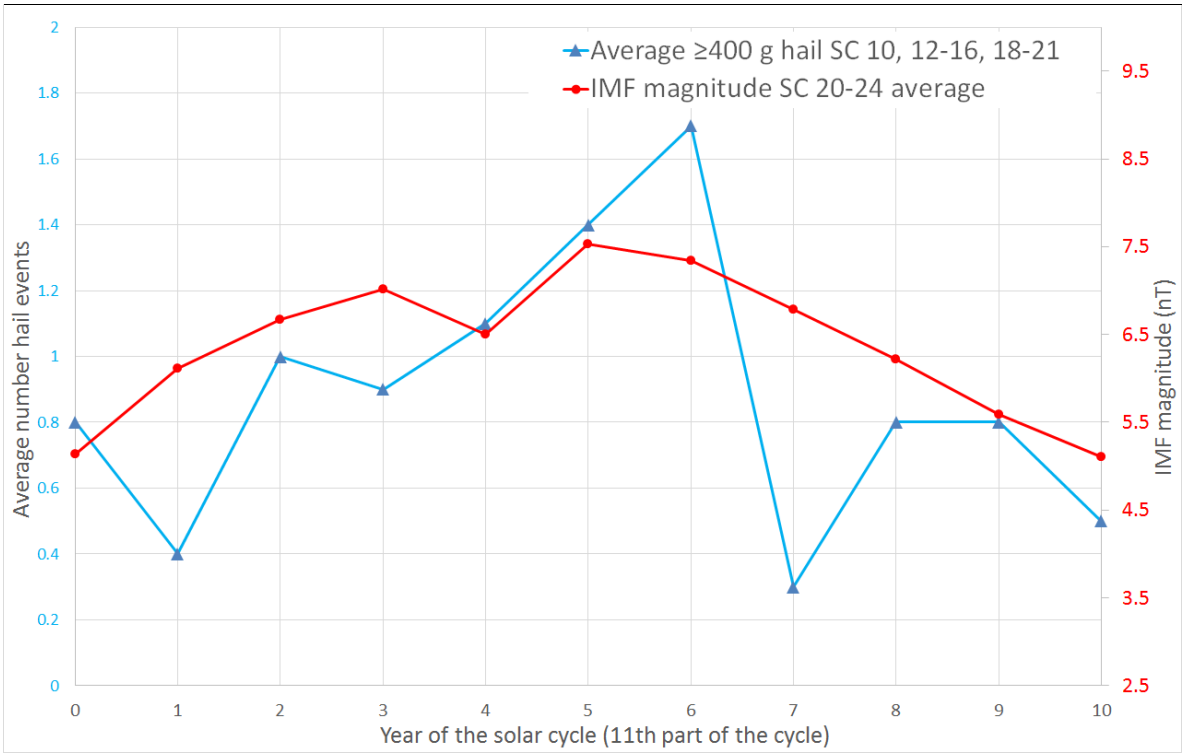

Figure 8 - *≥400 g hail events reported in newpapers are assigned to the 11th of the solar cycle (year of an idealized 11-year solar cycle) in which they take place, and the total count for each 11th across all cycles summed and plotted together with dynamic pressure (figure 7) and IMF magnitude (figure 8). Excluded cycles*

are those with incomplete data due to wars, or the last 3 solar cycles where weight reports have been replaced by diameter measurements and media.

3.4. Discussion and conclusions

Large hail in Spain seems to experience a cyclic variation in frequency related to the 11-year solar cycle. The IMF magnitude in particular matched relatively well the hail counts. However, as mentioned earlier, my objective is not to find the extent to which different space weather factors influence weather/volcanism, just to show evidence supporting a general connection.

Since large hail seems to be positively correlated with certain solar wind parameters, I think the mechanism where solar wind enhances hail activity may be similar to the mechanism where solar wind enhances volcanism. As seen in the earlier section 3, volcanic activity increased during and following years 2003 and 2015, which were the peaks in the IMF magnitude of their cycles. Seemingly both volcanism and large hail activity (assuming Spanish hail data to be representative of large hail as a whole) are positively correlated with solar wind/space weather activity in the near-Earth environment. Suggesting both phenomena may be part of the same large, complex interaction between solar wind and the Earth system, justifying the inclusion of such disparate phenomena as hail and volcanoes in the same article, since they may not be as unrelated to each other as they seem at first glance.

4. Decadal interrelated variations in weather, volcanism, and solar activity

4.1. Introduction and observations

The apparent link between solar activity and volcanism, and solar activity and weather, made it worthwhile to start looking at changes in volcanic and weather patterns on a decadal timescale as a function of variations in solar activity. While data on solar wind parameters is limited to the last few decades, data on solar sunspot numbers extends back over 300 years. Additionally, I think coordinated behavior between volcanic activity and large Spanish hail may reflect the changing solar wind conditions or changes in the Earth's reaction to it. Because of this, looking at the behavior of volcanoes and weather seemed a promising endeavor.

While compiling large hail events described in Spanish newspapers, it quickly became obvious that some years or decades featured extraordinary clusters of hail events. Exceptional clusters in large hail weight and number are seen in approximately 1944-1952, and 1884-1904 (see appendix), which also seemed correlated with periods of increased hurricane activity in the Atlantic (see section 4.3.2). One characteristic is that ≥400 g hail events over the well-described central Spain area (in the Ciudad Real, Toledo, Madrid, and Guadalajara provinces) were, since 1870, entirely limited to the 1890-1907, and 1949-1959 intervals that roughly match those two peaks. Preliminary investigation also indicates a possibly greater peak of large hail in central Spain in 1834-1847, likely associated with a series of extreme, poorly-known weather events over in Spain in 1826-1835, interrupted by a reporting blackout during the First Carlist War (1833-1840). The 1826-1835 cluster in Spain includes events such as the 1826 Canary tropical cyclone, which is considered to be the worst natural disaster in the Canary Islands in its 5 centuries of history (Bethencourt et al., 2008); the 1828 Tarragona hailstorm (D de B., 1829), which is likely the largest Spanish hail event in a Spanish province capital; or the 1835 Menorca tornado (Moragues, 1835), which to my knowledge would be the longest-tracked Spanish tornado and among the most damaging ones; among other remarkable weather events.

These extreme weather clusters took place at roughly regular intervals, suggesting a periodic behavior. For the 18th century, data is very incomplete, but the destructive hailstorms that hit Madrid during this century in 1736, and in 1782 and 1787 ("Quien debe pagar los vidrios rotos", 1899) possibly cluster around two earlier such peaks. ~1735, ~1785, ~1835, ~1890, ~1950, would correspond to roughly periodic peaks at 50-year intervals that have caught my attention. Another peak would be expected to have taken place around the year 2000. While in terms of hail I'm not entirely sure if there was one, as will be discussed later other parameters shed light on this last peak.

4.2. Data and methods

To study more closely how volcanism has evolved over decadal timescales I had to judge variations in volcanic activity. One problem however is that many volcanic regions of the world may have incomplete eruption records until very recently. Another is that the information that does exist is mostly limited to the occurrence of eruptions, with relevant data such as the nature of the activity being mostly absent. Lastly, it became evident while looking at the data, that different types of volcanism may have evolved differently over time. My strategy was to rely on volcanic regions with a more complete, trustworthy eruption record. Regarding types of

volcanism, three main classes of volcanic activity are related to the tectonic setting, that is mid-ocean ridge, subduction zone, and intraplate volcanism. These three settings generally correspond to the main three families of magma chemistry, mid-ocean ridges erupt subalkaline magmas, subduction zone cal-alkaline magmas, and intraplate settings alkaline magmas, save exceptions.

4.2.1. Mid-ocean ridge/subalkaline volcanism

Mid-ocean ridge volcanism takes place where tectonic plates are pulled apart underwater and a new oceanic floor is created. This kind of volcanism is poorly documented, and I think very difficult to gauge how it has evolved over time, despite being possibly the most voluminous form of volcanism but due to being underwater it goes unobserved. Two exceptions may be Iceland and Afar volcanic regions. However the latter, due to remoteness and little-known eruption history, is not a suitable target. Iceland is more promising, but I've still left it out due to the subglacial volcanoes of Iceland having uncertain eruptions, or incomplete eruption histories. Chemically there are other occurrences of subalkaline volcanism outside mid-ocean ridges, for example, Hawaii is largely subalkaline in chemistry (Sherrod et al., 2021).

4.2.2. Subduction-zone/calc-alkaline volcanism

Subduction-zone volcanism occurs when an oceanic plate collides with another plate, oceanic or continental, one plate is subducted and a chain of volcanoes develops over the subducted plate. Regarding subduction zone volcanism I've decided to look at Japan. Japan has a prolific history of volcano monitoring. Continuous observation of volcanism by the Japan Meteorological Agency started as early as 1888 and the first volcano observatory was established in 1911 (Yamasato, 2005). Additionally, the Japanese nation has over a hundred active volcanoes so it may be an ideal target to study how subduction-zone volcanism has evolved historically. I think the eruption record of Japanese volcanoes may be fairly complete since monitoring started in 1888, or at least by the early 20th century when a vast national telegraph network was in place (Arai, 2019). This is probably much more complete information than other major subduction zone volcanic regions. I obtained data from the National Catalogue of the Active Volcanoes in Japan (Japan Meteorological Agency, 2013). I excluded from the analysis the Bonin, Mariana, and Kurile islands, due to being remote and likely more incomplete regarding eruption records than the rest of the country. Yearly totals of erupting volcanoes are an ideal way of judging subduction zone volcanism because volcanoes in these settings can produce semi-sustained activity and there will be multiple erupting volcanoes per year in Japan, sometimes even erupting for decades on end.

4.2.3. Intraplate/alkaline volcanism and subalkaline intraplate Hawaiian volcanism

Intraplate volcanism includes volcanic regions away from plate boundaries. Intraplate eruptions are generally fissure eruptions fed from sheet intrusions (magma-filled cracks), of medium duration (days or months generally), and involving the formation of a new lava flow. For some volcanoes, eruptions might roughly represent a lava volume unit since lava flows may have a similar size in each eruption. Because of this, I've decided to look at eruption counts per year for several intraplate volcanoes put together. I have included the Canary, Azores, and Cape Verde Islands, which have very complete eruption records that reach back to before 1600. I have included the Comoros, Samoa, and Cameroon Line volcanic provinces, which seem to have very complete eruption records back to around 1850. All these volcanoes are alkaline in composition and consist of voluminous shield volcanoes built from overlapping lava flows. Data used comes from the Global Volcanism Catalogue (Venzke, 2024).

Hawaii is another important intraplate volcanic province, and unlike other such areas erupts magma with a subalkaline chemistry. The information is particularly detailed in this case, so I've tried to approximate the magma influx rate over time by using the following method. A dike intrusion and/or eruption results in magma being retrieved from the volcano, magma influx eventually resupplies the volcano resulting in another eruption. The resupply should be around the same scale as the volume involved in the previous dike/eruption event. I assume that in between magma retrieval events (dike intrusions and/or eruptions), the magma influx rate is that of the volume of the first event divided by the interval between the two events. This is a rough approximation of magma influx rate but I think it's the best that can be done with the data I can access. Another scenario is that of long-lived eruptions that occur in equilibrium with magma supply, during such eruptions the volcano does not experience rapid deflation/subsidence that corresponds to magma being retrieved from the volcanic storage. In such events, I consider the influx to be the eruption rate. Such eruptions in equilibrium with supply include the following Kilauea eruptions: caldera filling during much of the 19th century and early 20th century, the Mauna Ulu eruption (1969-1974), and the Pu'u'o'o eruption (1983-2018).

For Kilauea, I've used data from Wright and Klein, 2014. The data provided by Wright and Klein extends to 2008, so I've only analyzed the period until 2008. I use tilt volume estimates provided in this publication which account for the total magma volume retrieved from Kilauea's storage as a result of both eruptions onto the surface and intrusions into sheet intrusions underground, the erupted volume is corrected for 20 % vesicularity following their approach. For Mauna Loa, the other subaerial, active Hawaii volcano during this interval, I use eruption volumes provided by Lockwood and Lipman, 1987. I approximate the volume of dike intrusions of Mauna Loa (not given by Lockwood and Lipman) by assuming a 2-kilometer height, 2-meter width, and a length enough to reach the lowest fissures during each eruption, values that are similar to more recent well-studied Hawaiian dike intrusions (Montgomery-Brown et al., 2010; Lundgren et al., 2013). With this data, and using the approach described, magma influx into Hawaiian volcanoes is approximated. Some factors are not included such as net inflation or deflation across eruptions/dike intrusion cycles or deep rift spreading but it still should be enough to form an approximate idea of the ups and downs of magma influx/production in Hawaii, which is representative of an intraplate subalkaline volcanic province.

4.2.4. Weather variables

Regarding hail activity, I will be using the ≥400 grams hail events that are listed in the appendix. But I also wanted to look at hurricanes. Vinós, 2024, shows a correlation between solar cycles and major hurricanes, with major hurricanes peaking after the sunspot maximum during solar cycles 21, 22, 23, and 24. This follows a very similar pattern to hail activity and volcanism, as seen previously. My thoughts were that hurricane activity could be modulated by a similar mechanism as Spanish large hail and volcanic activity. To compare hurricane activity to the other variables I looked at accumulated cyclone energy (ACE), a measure of the overall activity of tropical cyclones during a hurricane season. I obtained ACE data for the North Atlantic from Wikipedia (Atlantic hurricane season, 2024), which in turn is obtained or adapted from the HURDAT database of the National Hurricane Center (Landsea and Franklin, 2013). I do not know much about the completeness of this database for old periods, but it can be used nonetheless to identify decadal peaks in hurricane activity.

4.2.5. Sunspot number

The sunspot number is probably an indicator of how solar activity has evolved since 1700. While near-Earth solar wind parameters tend to peak later in the 11-year cycle than sunspot number, both of these solar wind parameters are higher in cycles with higher sunspot numbers. For example, in the period covered by OMNI data, since 1965, the highest values of proton density and IMF magnitude were reached in solar cycles 21 and 22, which also reached the highest yearly sunspot numbers of this period. Even if sunspot number and near-Earth solar wind parameters peaked at different times within the cycle they all do seem to mirror the variations between different cycles. So the analysis will rely on sunspot numbers. I will use yearly sunspot number average data from the Solar Influences Data Analysis Center of the Royal Observatory of Belgium (SILSO).

4.3. Results

4.3.1. Positive correlation between sunspot number and Japanese volcanism

Figure 9 plots Japanese erupting volcanoes and sunspot number vs time using 11-year averages of erupting volcanoes to smooth the line. As can be seen, Japanese volcanism seems to be roughly proportional to the maximum sunspot numbers reached in each 11-year solar cycle. This seems in line with the observed positive correlation between magma influx into volcanoes and solar wind during cycles 23 and 24 discussed in section 2, or the modulation of Kilauea volcano activity by the IMF Bx component discussed in section 1. Showing a strong control of solar activity over volcanic activity on Earth. The most active years are 1954, 1959, and 1962, with nine erupting volcanoes in Japan.

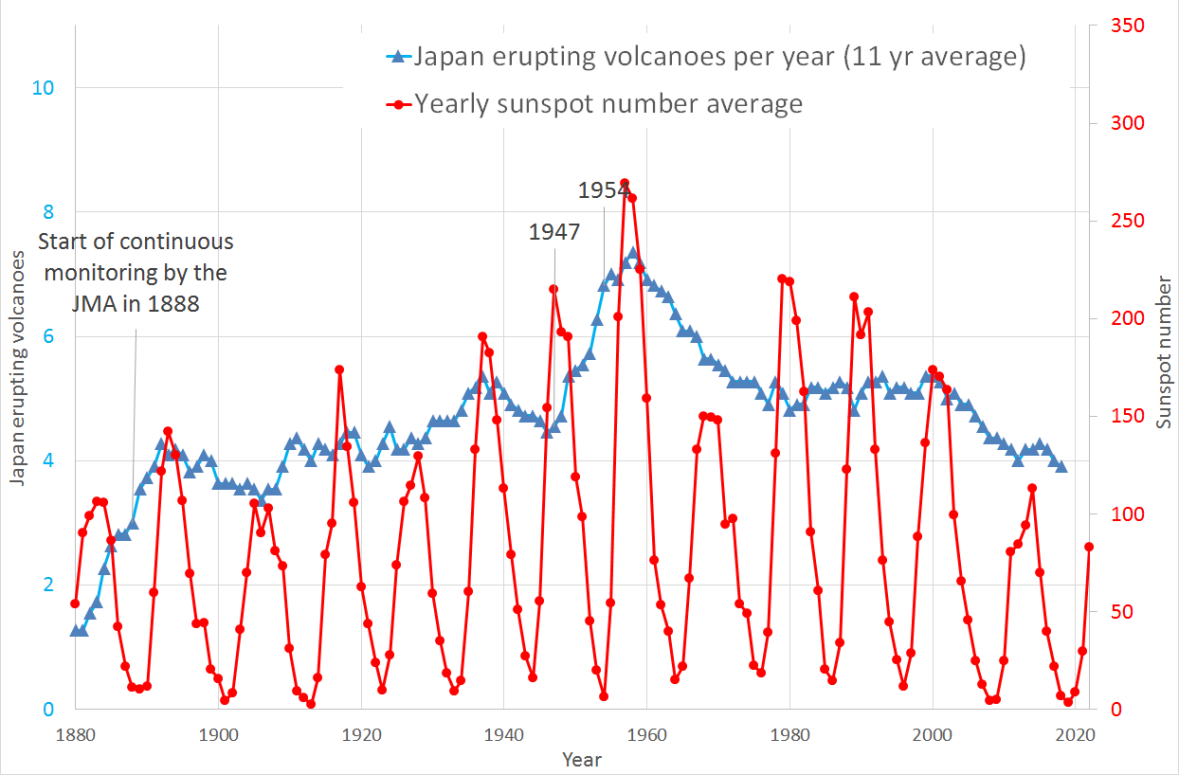

Figure 9 – Japanese number of erupting volcanoes per year exclude the Kurile, Bonin and Mariana islands which are remote, in order to exclude incomplete data. The increase in volcanism at the start of the graph is likely to be influenced by the start of volcano monitoring by the JMA. Multiple eruptions of the same volcano in one year only count as one, so that repeated small scale phreatic or vulcanian activity doesn't skew the data.

4.3.2. Positive correlation between Spanish large hail and Atlantic ACE

Figure 13 plots Atlantic accumulated cyclone energy, and yearly count of ≥400 g hail per year, both convective weather phenomena. A pattern is apparent where both variables are positively correlated. Both variables seem to have major decadal peaks around 1893 and 1949. A third 2005 hurricane peak may be associated with a smaller peak in ≥400 g Spanish hail around 2006. The 50-year cycle or oscillation seems visible in both ≥400 g Spanish hail and North Atlantic hurricane activity, and the peaks occur roughly simultaneously across both variables. Unlike in hail, however, there is a long-term increase in ACE. Since I do not know how complete the HURDAT database is, it's hard to know whether this increase is due to improved monitoring or not.

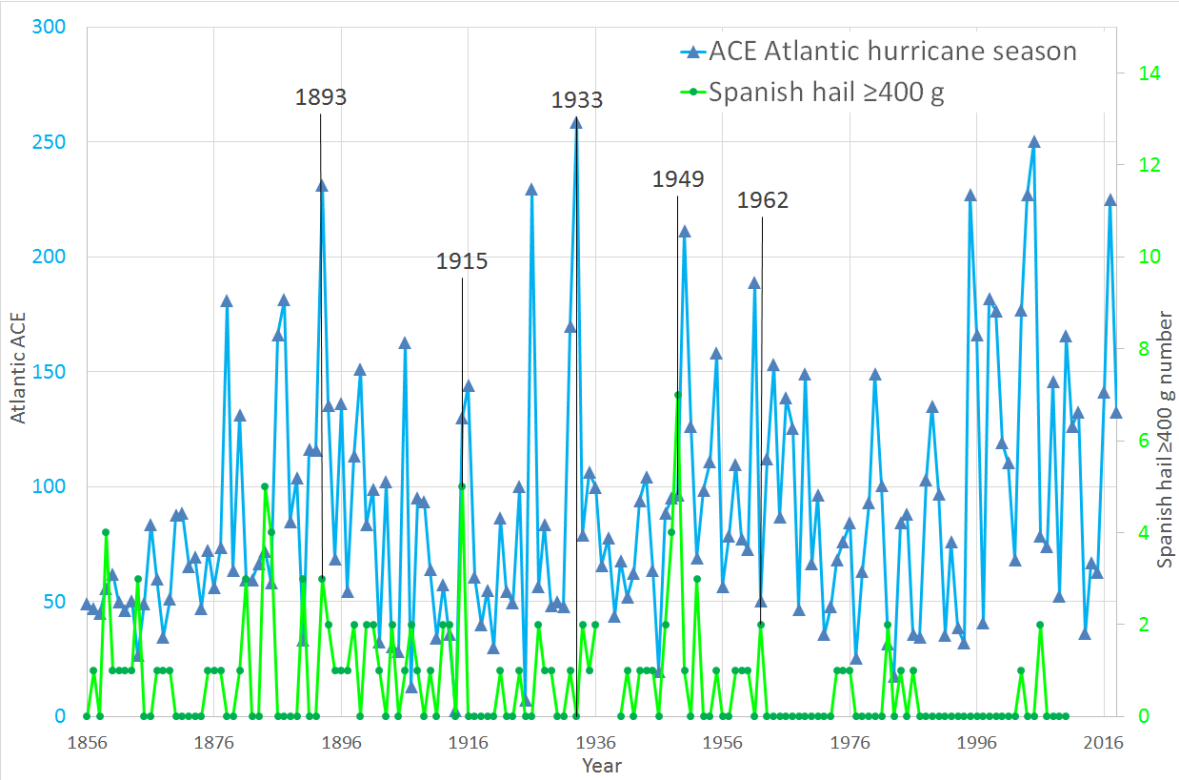

Figure 10 – *Atlantic accumulated cyclone energy and hail event counts per year.*

4.3.3. 50-year cycles in alkaline intraplate volcanism and relation to Spanish hail

Table 2 and Figure 11 show the activity in the Azores, Cameroon, Canary, Cape Verde, Comoros, and Samoa volcanic provinces, which I considered representative of terrestrial intraplate alkaline volcanism. Activity seems to rise and fall every 50 years showing a similar period to the possible cycles seen in Spanish large hail and Atlantic ACE, and with roughly coincident peaks. This cycle is not controlled by solar activity, or at least it does not look this way. Figure 12 compares the alkaline volcanism per year averaged for 11-year intervals with sunspot number. The four major pulses have taken place during both times of high and low solar activity, so they do not seem directly controlled by the Sun. I do think however, because all these variables have shown some link to solar activity, and because it would otherwise be difficult for phenomena in the atmosphere and geosphere to be connected, that the 50-year cycles may have to do with the way the Earth responds to solar activity, in the processes that involve transfer of energy from solar wind to terrestrial phenomena.

Peaks in intraplate alkaline volcanism took place around 1862, 1906, 1952, and 2003. The first peak is unclear, but the following three match the major peaks in ≥400 g Spanish hail and Atlantic ACE. Figure 13 plots ≥400 g Spanish hail vs intraplate alkaline volcanism. I do think however that the alkaline volcanism peaks take place towards the end of periods of elevated hail activity. Hail was already very elevated from 1880 onwards, yet alkaline volcanism only started to visibly increase after 1900. The same may happen in the following period. Although hail activity is very focused around 1949, the 1936-1939 period is entirely lacking in hail information due to the disastrous Civil War, and in later years the information I believe is also very incomplete, with a larger proportion of total reports referring to province capitals. This is not something I can confidently answer yet, but based on large hail occurrences in province capitals, I suspect hail levels by 1930 were already close to those in 1950, and that activity may have peaked somewhere in between.

Eruptions of alkaline "oceanic" volcanoes since 1830	
Province	Volcano (eruptions)
Azores	Sete Cidades (1861, 1880), Terceira (1867, 1998), Sao Jorge (1902), Monaco Bank (1907, 1911), Fayal (1957)
Cameroon Line	Santa Isabel (1898, 1903, 1923), Mt. Cameroon (1838, 1852, 1865, 1866, 1871, 1909, 1922, 1925, 1954, 1959, 1982, 1989, 1999, 2000)
Canary	Tenerife (1909), La Palma (1949, 1971, 2021), El Hierro (2011)
Cape Verde	Fogo (1847, 1852, 1857, 1909, 1951, 1995, 2014)
Comores	Karthala (1830, 1833, 1848, 1850, 1855, 1857, 1858, 1859, 1860, 1865, 1872, 1876, 1880, 1883, 1904, 1910, 1918, 1928, 1948, 1952, 1956, 1965, 1972, 1977, 1991, 2005 (Apr), 2005 (Nov), 2006, 2007)
Samoa	Ofu-Olosega (1866), Savai'i (1902, 1905)

Table 2 – The above table shows a list of eruptions in the volcanic provinces selected for the period since 1830, which are represented in figure 11, and ploted as multi-year averages in figures 12-13.

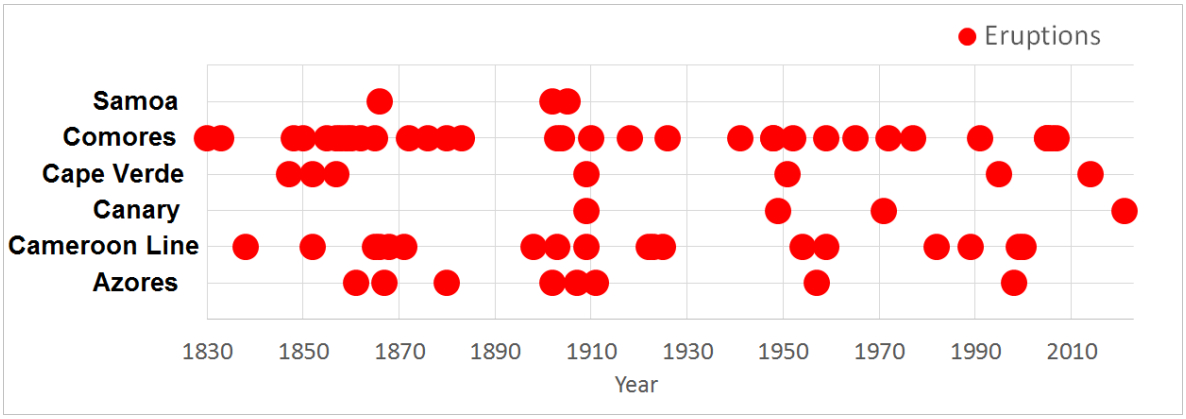

Figure 11

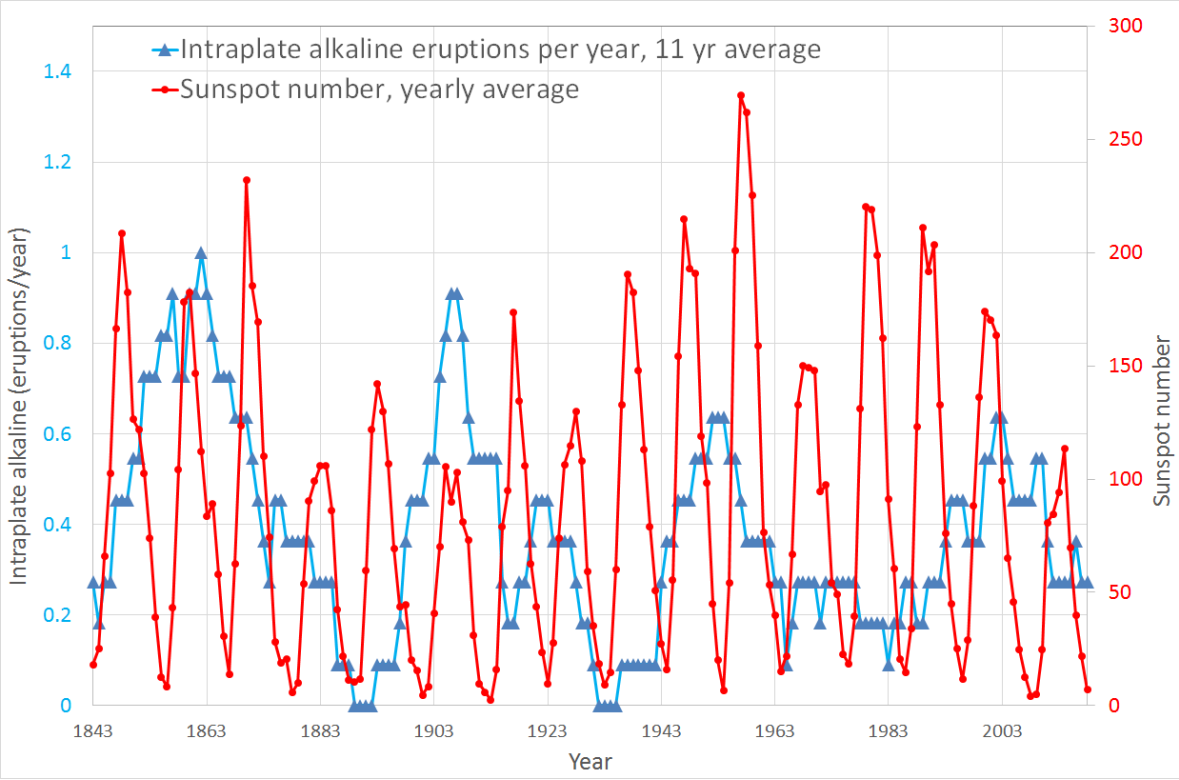

Figure 12

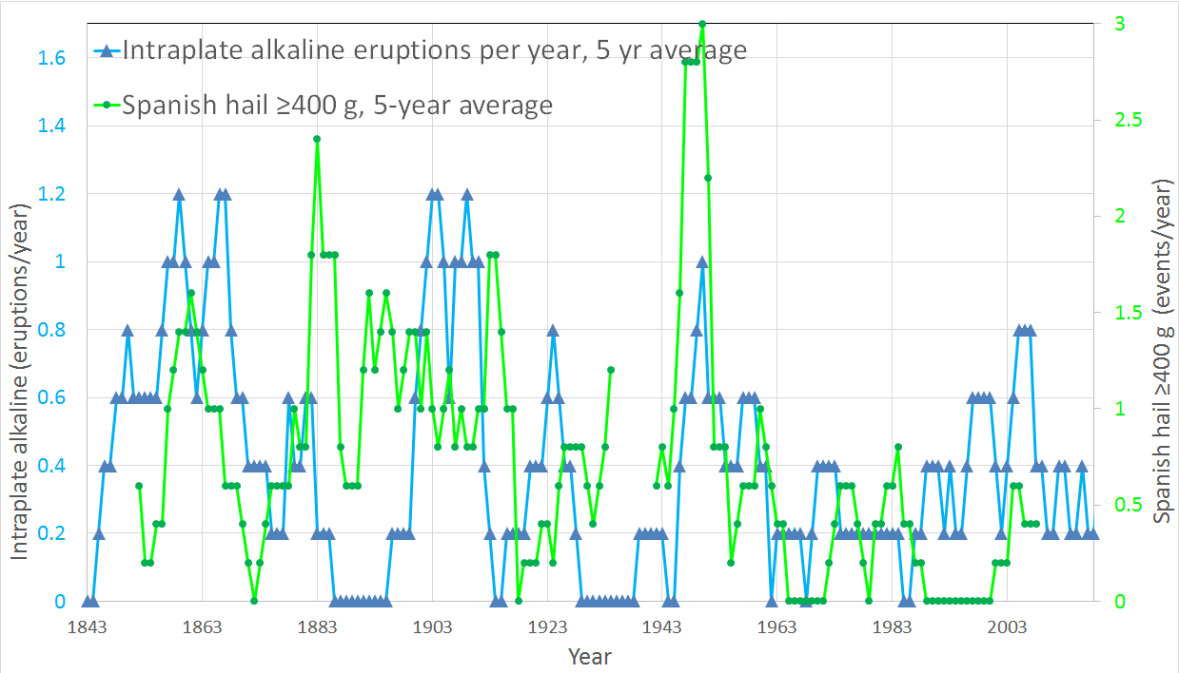

Figure 13

4.3.4. Negative correlation between Spanish large hail and Hawaii volcanism

One of the more interesting results when comparing the data was finding a very apparent negative correlation between the magma influx into Hawaiian volcanoes and large hail in Spain. Interesting questions like why large hail activity in Spain dropped so sharply around 1960, or why Hawaiian volcanism has been so intense in the past few decades, may be two pieces of the same puzzle, and help answer this question and enlighten on their inner workings. Peaks in the estimated Hawaiian magma influx seem to be associated with lows in the large hail activity over Spain, and lows in magma influx to peaks in the large hail activity (figure 14). The major peaks in large hail around 1890 and 1950 take place during times when the Hawaii magma influx was very low, in the 1890s possibly at the very lowest. A major transition in activity, from Mauna Loa to Kilauea, and to the East Rift Zone of Kilauea, in the 1950s, seems to take place with little change in magma supply, but after 1960 the influx rapidly rose.

Between 1960 and 1980, a very important change seems to take place that marks a before and after in Spanish hail and Hawaiian volcanism. And since both of these parameters may be indicators of major processes taking place on a global scale, then this could have major implications. Hawaii's magma influx strengthened around 1960 and further after 1980 and has probably remained extremely elevated to the present day. The data, based on Wright and Klein, 2014, only covers until 2008, but sustained lava effusion at about the same rate continued to 2018. And after the breakdown of the continuous activity in 2018 there have still been frequent eruptions and very high deformation rates. So this era of high supply probably continues at present, whether at the same level or not will require the proper estimations.

This 1960-1980 change in magma supply to Hawaii matches with a spectacular collapse in large hail activity over Spain, in terms of frequency but also size, given that hailstones before 1960 often reached weights of 1.5 kg or above, but, after 1962, the much fewer hailstorms that exceeded 400 g barely made it to this size, most of them having 400-500 g in weight. Apart from a doubtful report in 2006, only a 2003 storm has reported values that are comparable to those that, before 1960, happened multiple times every decade (except for the 1930s which however have a very incomplete record due to the Spanish Civil War)

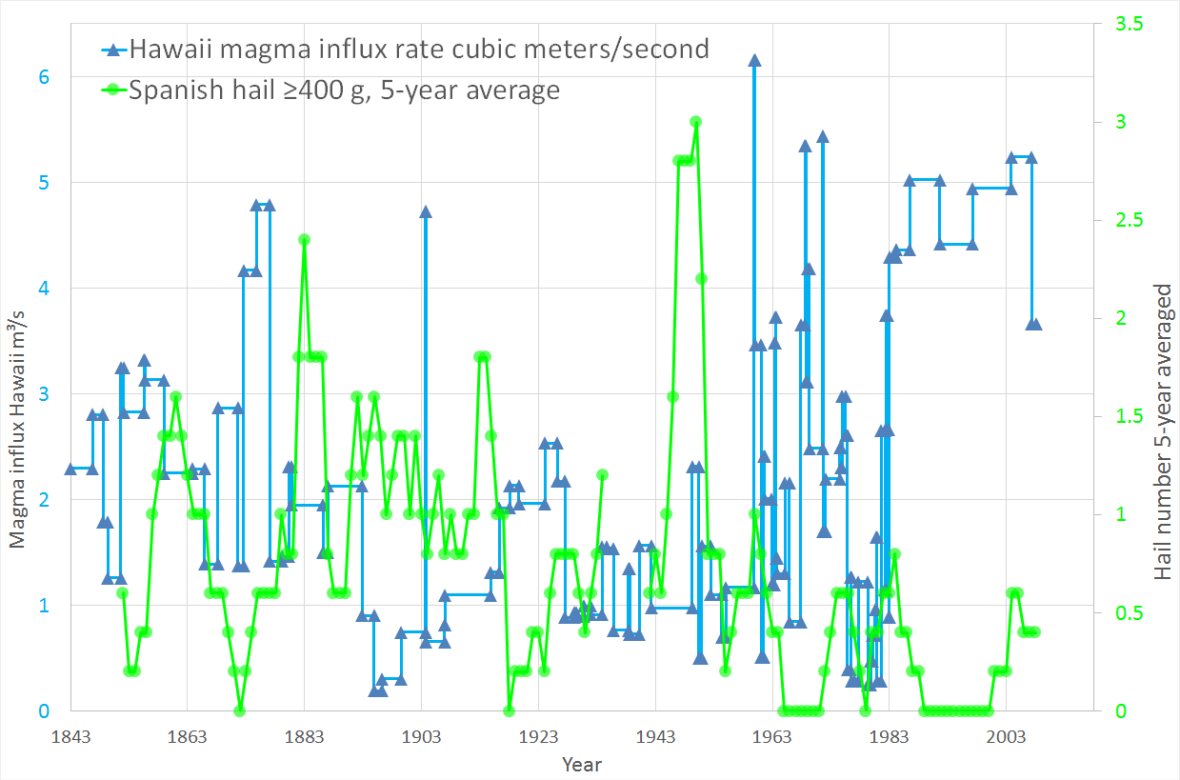

Figure 14 – Hawaii magma influx rate is calculated for intervals of time in between Kilauea or Mauna eruptions or sheet intrusions, or intervals of continuous effusion with a known output. Data sources are described in section 4.2.3.

5. Alkaline and calc-alkaline magma chemistry review.

5.1. Introduction to magma chemistry

Before I discuss the mechanism behind the solar-weather-volcanism connection I think the chemistry of magmas may be one more important piece of evidence to consider.

Magmas come in a great variety. They have different elemental compositions and the source of this variation has been a matter of much interest. One question is how magma acquires this diversity. A well-known process is fractional crystallization, in which, as magma cools, part of it starts to solidify crystallizing into various minerals. The minerals that crystallize from the melt have different chemical compositions from the original magma, and when they are left behind, the new magma has a different chemical composition to the original (Bowen, 1956). This process takes place during the journey of magma within the Earth when it stagnates and cools before reaching the surface. As such magma will make a series of chemical compositions from a primitive magma to an evolved endmember by subtracting a solid fraction as it cools.

5.1.1. Subalkaline, alkaline, and calc-alkaline

Apart from crystal fractionation, there is more variety in magmas. There exist mainly three different suites, usually known as subalkaline, alkaline, and calc-alkaline; which are largely related to specific tectonic settings, mid-ocean ridge, intraplate, and subduction zone environments respectively. Table 3 shows the composition of some representative magma types, all of which are primitive, or near-primitive magmas as considered by the original sources, and as indicated by high MgO content within their suite. If we are dealing only with primitive magma types in or above 6 wt% MgO, the SiO2 content is possibly the best indicator of the suite the magma belongs to.

Whole rock major oxides (wt%) in representative magma types										
Type	SiO2	TiO2	Al2O3	FeOT	MnO	MgO	CaO	Na2O	K2O	P2O5
1. High-Mg andesite	56.32	0.67	17.17	5.05	0.11	6.22	7.45	3.60	1.21	0.15
2. MORB subalk.	48.18	0.87	15.89	8.43	0.17	10.12	12.95	1.75	0.08	0.06
3. Melt experiment	**48.07**	**0.58**	**15.92**	**7.54**	**0.15**	**12.35**	**13.72**	**1.38**	**0.14**	
4. Intraplate subalk.	49.95	2.53	12.78	11.26		9.69	10.51	2.18	0.45	0.21
5. Intraplate alkaline	41.68	2.93	11.54	12.04	0.19	14.11	9.96	3.46	1.45	0.87
6. Alkaline continental	35.84	2.46	8.11	9.96	0.20	18.30	15.81	1.69	0.99	0.90

Table 3 – Type 1 is a subduction-zone high-magnesium andesite from Piip volcano in the Bering Sea, data is from Yogodzinski et al., 1994. Type 2 is a mid-ocean ridge subalkaline basalt from Grjothals in Iceland, data is from Slater et al.,1998. Type 3 is an artificial melt produced in a melting experiment of depleted peridotite, meant to illustrate the similarities between subalkaline basaltic melts and partial melting of peridotites, this particular example being 2.6 wt% melting of depleted peridotite at 10 kbar and 1290 °C from Wasylenki, 2003. Type 4 is an intraplate subalkaline basalt from Kilauea volcano, one of the most magnesian glass compositions of the volcano, found among the Keanakakoi tehras, from Lynn et al. 2017. Type 5 is an intraplate alkaline magma from Lanzarote Island in the Canary Archipelago, it's a basanite erupted in September 1730, from Carracedo, Rodriguez, and Soler, 1990. Type 6 is an alkaline melilitite magma from Urach volcano in Germany, from Wilson et al.,1995; Hegner et al., 1995; and Alibert et al,1983.

5.1.2. Subalkaline magma

The subalkaline lavas erupted in mid-ocean ridges, where tectonic plates separate and material emerges from below, tend to have 48-50 wt% SiO2 values. Such magmas are generally referred to as subalkaline or tholeiite basalts. Type 2 magma (from table 3) is from Grjothals, Iceland (Slater et al. 1998). It is a particularly primitive case of mid-ocean ridge basalt, with very low TiO2 and FeOT (these oxides can increase at constant silica through plagioclase-augite crystal fractionation). Type 3 is a partial melt experiment conducted in depleted peridotite, the likely most typical composition of the Earth's mantle, where 2.6 wt% of a depleted peridotite was melted and the chemical composition of the resulting liquid was analyzed (Wasylenki, 2003). Among the runs provided by Wasylenki, I chose 2.6 wt% melting of a peridotite because it seemed closest to the composition of Grjothals. As can be seen, types 2 and 3 (the Grjothals basalt and the 2.6 wt% melt of a depleted peridotite) are very similar in chemistry in every major oxide. Supporting the notion that mid-ocean ridge magma comes from the melting of a peridotite mantle.

5.1.3. Alkaline magma

Types 5 and 6 in Table 2 are representative examples of alkaline magmas. Alkaline magmas are typical of intraplate volcanic environments. When dealing with magmas above 6 wt% MgO alkaline magmas can be distinguished by having less than 48 wt% SiO2, as is the case for the examples given, which are both well into the alkaline field. Alkaline magmas get their name from the high concentration of the alkali metals sodium and potassium, although this may be a misleading name, both because it can get confused with other chemistry concepts and because the high sodium and potassium are more prominent in evolved alkaline magmas than primitive, in which sodium, can actually be depleted, as is the case for type 6.

Type 5 is a type of magma known as basanite, from the start Timanfaya eruption that we will see later in more detail (Carracedo et al., 1990). Type 6 is the average of Urach volcanic field samples provided by three studies (Wilson et al., 1995; Hegner at al., 1995; Alibert et al, 1983). All Urach samples are extremely alkaline, which can be seen in their extravagant composition, with as low as 36 wt% SiO2 or 8 wt% Al2O3, or as high as 18 wt% MgO or 15 wt% CaO, which are concentrations extremely different from those of typical basalts.

5.1.4. Calc-alkaline magma/high-magnesium andesites

The calc-alkaline magma suite is considered to be characteristic of subduction zone volcanism (where plates converge and an oceanic plate subducts into the mantle), its chemistry is variably defined but one of the common ways of discriminating them is using FeOT/MgO versus SiO2 diagrams, where calc-alkaline magmas have lower FeOT/MgO ratios and higher SiO2 contents than sub-alkaline magmas (Miyashiro, 1974). This refers to a frequent characteristic of subduction zone magmas, having high silica and low iron and calcium oxides for a given level of magnesium oxide, often known as high-magnesium andesites.

Type 1 is an end-member example of such a magma from Piip volcano in the Bering Sea, a submarine stratovolcano located along the convergent boundary of the Pacific and North American plates. The Piip lavas exhibit high SiO2, low CaO, and FeOT (Yogodzinski et al., 1994) and are considered to be high-magnesium

andesites (magnesian andesites). In many ways, calc-alkaline/high magnesium andesites are the opposite to alkaline magmas, and I think this may be a very important aspect to keep in mind.

The TiO2, FeOT, MnO, CaO, and MgO depletion in Piip lavas seem opposite to the enrichment of these oxides in alkaline magmas like Urach or Timanfaya. The enrichment in SiO2 and Al2O3 is also contrary to the depletion of these oxides in alkaline magmas. The one common aspect in both types is enrichment in Na2O and K2O relative to subalkaline magmas. This is why I think that both magmas may be opposite end members of the same spectrum, this makes sense considering the law of conservation of matter, which implies that within a closed system if certain elements have become concentrated in a particular mass they must have been depleted from some other mass, and by this reasoning, it's possible that the elements that are more concentrated in alkaline magmas come from a depletion in calc-alkaline magmas, and vice-versa. That there is not a perfect match casts some doubt on this possibility, however if alkaline and calc-alkaline magmas are part of a broader system it is possible that both "steal" sodium and potassium from somewhere else, while alkaline magmas become enriched in titanium, iron, manganese, calcium and magnesium among other less important elements from a calc-alkaline magma depletion. More on this will be discussed later.

5.2. The Timanfaya eruption.

5.2.1. Introduction

The 1730-1736 Timanfaya eruption of Lanzarote in the Canary Islands, Spain, was very exceptional. This eruption may be a window into the processes that give rise to alkaline magmas. Timanfaya's uniqueness lies in several aspects: it's one the most voluminous eruptions of the planet in historical times, erupting 2.5-5 km3 of lava flows; it was exceedingly long-lived, lasting 2053 days of effusion; and it erupted unusual chemistry, starting with basanite, then erupting alkaline basalt, and finally subalkaline basalt (Carracedo et al., 1990). The order of the magmas was that of gradually decreasing alkalinity. All other historical eruptions in the Canary Islands have effused basanite magma, <45 wt% silica, or its evolved products like tephrite and phonolite, and none of these eruptions exceeded 0.3 km3 (Longpre and Felpeto, 2021; and references therein). In an almost entirely basanite volcanic province, to see the eruption of subalkaline basalts is highly exceptional, and even more to have an eruption that shifts across such widely different compositions as basanite, then alkaline basalt, and subalkaline basalt. This requires an explanation.

Some aspects of the Timanfaya eruption may be important. The first is that most silica-depleted basanite only erupted briefly from the first vent that opened, which lasted the first month. There was a rapid change towards less alkaline compositions. A few months into the eruption subalkaline lava was being effused and stayed that way until the end. Also, all lavas have very high MgO indicative of primitive composition. A second eruption of negligible volume, 0.01 km3 (Longpre and Felpeto, 2021), took place in 1824, which may be considered an after-eruption of the 1730-1736 event. This 1824 eruption produced basanite with 44 wt% SiO2, slightly less alkaline than the Timanfaya opening, but more so than the Timanfaya bulk basalt. Otherwise, Lanzarote has not erupted historically nor are there any other known Holocene eruptions. Chemical data from the different phases and the 1824 eruption is from Carracedo et al., 1990.

The average chemistry of the Timanfaya eruption opening month (September 1730) and 1731-1736 subalkaline basalt is shown in table 4. This is a perfect case in which to study the differences between alkaline and subalkaline because both magmas erupted in the same plumbing, setting, and mantle, leaving out many other variables that could interfere. It's a great way to isolate the alkalinity variable, looking at one same volcano, one same eruption even, that has erupted both types.

Looking at table 3, I would note that SiO2 and Al2O3 are more depleted in the Sep. 1730 basanite, while all the other major oxides are enriched in the basanite. The magma storage of Lanzarote Island must have contained basanite magma at the start of the 1730 eruption, this storage must have been relatively small and rapidly depleted by the voluminous Timanfaya eruption, drawing primitive magma from the mantle.

Whole rock major oxides (wt%) and initial/final ratio in Timanfaya lavas											
	SiO2	TiO2	Al2O3	FeOT	MnO	MgO	CaO	Na2O	K2O	P2O5	Cr (ppm)
1731-1736 basalt	48.89	2.46	13.45	10.80	0.15	9.39	9.38	3.22	0.65	0.33	499
Sept. 1730 basanite	41.68	2.93	11.54	12.04	0.19	14.11	9.96	3.46	1.45	0.87	694
Inital/late lava	0.85	1.19	0.86	1.12	1.27	1.50	1.06	1.07	2.24	2.61	1.39

Table 4 - *Initial/late lava divides the concentrations in the basanite in between the concentrations in the basalt to illustrate the possible changes that gave rise to the basanite. Data is from Carracedo et al., 1990.*

5.2.2. Current models regarding alkaline magma generation

Carracedo (1990) explains the changes in magma chemistry during the Timanfaya eruption as a function of melting degree, which is a formerly popular explanation for the origin of alkaline melts, that lower degrees of melting will yield more alkaline melts, and higher degrees subalkaline magmas. However, this idea has proven problematic due to some characteristics of alkaline magma, like having higher MgO than subalkaline magmas when experimental results show lower degrees of melting would lead to lower MgO concentrations in the melt, or Al2O3 being higher in experiments at lower melting degrees (Wasylenki, 2003) when alkaline magmas have lower contents. More recently other ideas have arisen.

More recent models involve the alkaline magmas being generated from an anomalous mantle, the most successful and growingly popular model involves partial melting from a carbonated peridotite. Melting experiments on peridotite plus carbon dioxide have been relatively successful in producing melts of similar composition to highly alkaline magmas. Table 5 shows two such experimental partial melts from scientific literature, which were obtained at 3 GPa pressure and 1350-1400 °C. Type 2 is from Dasgupta, Hirschmann, and Smith, 2007, and is relatively close to a Timanfaya basanite. Type 4 comes from Hirose, 1997, and shows a melt similar to an Urach melilitite. The difference is that in type 4 more CO2 was added to the melt than in type 2, with other conditions being similar, the melt turned out to be more extremely SiO2 and Al2O3 depleted. These aluminosilicate-depleted magmas therefore seem related to the presence of CO2, the more extreme the more CO2 is added to the melt. It seems natural to assume from these results that alkaline magmas originate from partial melting of a carbonated peridotite, but I suggest there may be other interpretations.

Comparison between alkaline lavas and melt experiments on carbonated peridotite									
Type	SiO2	TiO2	Al2O3	FeOT	MnO	MgO	CaO	Na2O	K2O
1. Timanfaya basanite	41.68	2.93	11.54	12.04	0.19	14.11	9.96	3.46	1.45
2. Peridotite+1 wt% CO2 melt	42.40	1.86	10.00	10.40	0.17	15.30	17.00	2.73	0.05
3. Urach melilitite	35.84	2.46	8.11	9.96	0.20	18.30	15.81	1.69	0.99
4. Peridotite+2.5 wt% CO2 melt	35.99	0.74	8.84	10.40	0.05	22.94	18.54	2.23	0.09

Table 5 – *Types 1 and 3 are natural Timanfaya and Urach lavas that have been discussed earlier. Types 2 and 4 are melting experiments on carbonated peridotite. Type 2 is from Dasgupta, Hirschmann, and Smith, 2007, and is relatively close to a Timanfaya basanite. Type 4 comes from Hirose, 1997, and shows a melt similar to an Urach melilitite.*

First of all, the melting of a carbonated peridotite is not a perfect explanation either. The experiments in the two publications mentioned earlier yielded melts that are very potassium-poor, none of the runs resulted in melts with more than 0.11 wt% K2O. In contrast, high potassium is one of the characteristics of alkaline magmas, with both Urach and Timanfaya having K2O contents of about 1wt% K2O or higher, a substantial difference. Other differences in TiO2 or CaO in the experimental vs natural melts are also significant.

However, I consider the distribution of alkaline volcanism is even more important. If alkaline magmas are produced from the melting of carbonated peridotite, then this composition must be present wherever alkaline volcanism takes place. The problem with this is that alkaline magmas are widespread in intraplate environments (Brenna, 2021 and references therein). Yet magmas such as basanites or melilitites have not been reported in mid-ocean ridges, where the mantle undergoes partial melting. If alkaline magma originates from carbonated peridotite mantle, and alkaline magmatism is very widespread then that means carbonated peridotite mantle should be widespread too, and chances are it would end up melting in mid-ocean ridges producing highly silica-depleted magmas such as basanites or melilitites. Yet, as far as I've been able to find, such silica-depleted magma compositions have not been reported from mid-ocean ridges, despite the extensive sampling of the latter.

5.2.3. Alkaline magmas as a form of magma differentiation

I theorize that alkaline volcanism is so widespread in intraplate environments because it can originate from a normal mantle, that typical subalkaline compositions, either melted from the mantle or recycled from subducted oceanic crust can be transformed into alkaline melts. I think that during the Timanfaya eruption, the first magmas erupted had differentiated from a subalkaline melt within the storage of the volcano, but due to voluminous effusion this differentiated melt was rapidly exhausted, and replaced by the original subalkaline melts rising from the asthenosphere. Timanfaya is not an isolated case either, alkaline magma followed by the

eruption of subalkaline magma is also documented in at least two other cases; the monogenetic (formed in one eruption) Udo volcano (Brenna et al., 2010) and Rangitoto volcano are reported to have erupted alkaline basalt followed by subalkaline basalt. However, I would argue that given the composition reported (Brenna et al. 2010 and 2011) the Udo case is alkaline basalt followed by eruption of calc-alkaline basalt, given that the late lavas are very silica-rich and also taking into account that the volcanic field where Udo erupted is in the back-arc of a subduction zone. It may be a common occurrence for eruptions to start with alkaline magma and shift to subalkaline magma. The other way around has not been reported. This particular behavior would be easy to understand if alkaline magmas originate from subalkaline or sometimes calc-alkaline magmas through differentiation.

If basanite was a differentiated product of subalkaline basalt it's easy to understand too why when Lanzarote Island erupted again in 1824 it produced a basanite that was very alkaline in composition, although not to the extreme of the first lavas of the 1730-1736 eruption. By 1824 basanite would have again built up within the small magma storage of Lanzarote Island, and since this eruption was minor it only erupted this differentiated basanite without drawing magma from the asthenosphere. The 1730-1736 event erupted 2.5-5 km3 of lava, while the 1824 event erupted only 0.01 km3 (Carracedo, 1990; Longpre and Felpeto, 2021). The dormancy to 1824 was relatively short and supply was probably more elevated in the aftermath of the Timanfaya eruption, so the composition did not become so extreme as in the much longer quiescence before the eruption in 1730.

6. Proposal. Electric currents induced by solar-wind-driven magnetosphere deformation as a mechanism driving the genesis of alkaline and calc-alkaline magmas, and modulating volcanism and "wet weather". Internal cycles in the geosphere modelating shifts in the location of induced currents within the planet.

6.1 Induced currents in the Earth modulating weather and volcanism.

The data shown in sections 1, 2, 3, and 4 support a very important link between solar wind conditions and at least some volcanic and weather phenomena. There must be a mechanism involved. Given that volcanic activity is modulated by the Bx component of the IMF on very short timescales, this narrows down the mechanism. It points to an electromagnetic process. The generation of magma implies an increase in the temperature of rock or partial melt, so that it can melt or melt further. An electromagnetic process that heats a material is required, this makes induction heating the most reasonable culprit. Induction heating consists of the heating of an electrically conductive material by electromagnetic induction. Electric currents are generated in the material when exposed to a time-varying magnetic field, and these currents disperse energy in the form of heat due to the resistivity of the material. Bullard, 1967, considered that induced electrical currents would be formed in the Earth's interior by changes in the Earth's magnetic field, the currents, according to Lenz's law, would be such that the magnetic field created by them opposes the change in the original magnetic field, and reduces this change within the conductor and its surroundings. Although they are a well-known process, their importance may have been underestimated and may need to be reassessed.

However, there is the issue of what would be the connection between solar wind and induced currents. There is a known, measured interaction between solar wind and the Earth's magnetic field. On Earth, for a given altitude, magnetic field strength is generally higher on the dayside than the nightside due to greater compression in the dayside magnetosphere by solar wind plasma flows (Li et al., 2020; Ju et al. 2016). As the Earth rotates, any given location periodically shifts between a dayside and nightside magnetosphere, with the corresponding change in magnetic field strength. Such locations will experience electromagnetically induced electric currents that produce a magnetic field opposing this change. The caveat is that I'm not capable of estimating if these changes would have the proposed effects or not. But I do think it would explain the link of weather and volcanic phenomena with the solar wind, given that seawater and magma are very conductive compared to other materials present in large amounts within the Earth, and because the magnetosphere deformation and ensuing induced currents would be expected to be stronger with more intense solar wind conditions, thus matching the observed positive correlation,

The mean conductivity of Earth's oceans is 3.31 ± 0.23 S/m, though it varies by as much as 0.0999–6.45 (S/m) depending on factors such as temperature and salinity, conductivity being higher in tropical latitudes than polar latitudes, and with more extreme variation at shallow depths (Tyler et al., 2017). The conductivity of a dry

basalt melt is also around 3 S/m (Zhang et al., 2021 and references therein) although will also vary depending on the temperature of the magma and water contents. In contrast crystalline unweathered igneous that make up most of the Earth's interior have conductivities of less than 0.001 S/m, and, save unusual rocks like massive sulfides or graphites, rocks stay in conductivity values that are well lower than those of seawater and magma (Best, 2015). As such, if induced currents are generated within the Earth, these currents would be expected to be particularly strong in seawater and magma.

Induction heating in seawater could favor phenomena such as hurricanes or hailstorms which are after all different forms of wet convection generated by hot, moist, unstable air masses rising through the atmosphere. Induction heating and/or enhanced evaporation may increase moisture over the oceans favoring more intense convective phenomena. This would fit with the observation of hailstorms peaking around the time of the near-Earth IMF magnitude peak. The connection is even more obvious for volcanism since induction currents in partial melt may elevate the temperature, increasing the melting degree, or melt the enclosing rock through thermal conduction, increasing the amount of generated magma, and as a result, the amount of erupted lava. Electromagnetic induction heating has already been proposed as a mechanism driving volcanic activity in some exoplanets (Kislyakova and Noack, 2020). This partial melt is most likely to be located in the asthenosphere, a globally widespread layer of partial melting at depths of roughly 150-100 km below the surface, that is supported by seismic evidence showing a layer of low seismic wave velocity and a gradient in velocity at its base (Hua et al., 2023).

6.2 Induced currents in magmas generating silica-alumina depleted and enriched melts.

An advantage to the notion of induced currents in magmas is that it may explain the chemical variability of magmas, and in particular the alkaline (silica-depleted) and calc-alkaline (silica-enriched) types.

Magmas (referring to silicate magmas) are ionic conductors, like seawater, where charge is carried by moving ions within the melt structure (Ni et al., 2015). Cations in the magma are divided into two groups, the network forming cations (Si and Al) and the network modifying cations (Na, K, Ca, Mg, Fe, and others), where the former construct polymers of linked silicate and aluminate tetrahedra that contribute to melt viscosity and are less mobile, while the later are more mobile and are the main charge carriers in the magma (Zhang et al., 2021). As such, network modifying cations should contribute more to electromagnetically induced electric currents than Si and Al. In general, I expect the majority of elements, trace elements, and rare earth elements should be more mobile than Si and Al in the magma structure.

As was discussed in section 5 the main difference between alkaline, subalkaline, and high magnesium andesite/calc-alkaline, is that of the amount of silica and alumina in the magma, with subalkaline melts having the concentrations expected from melting a typical mantle peridotite composition, while alkaline melts are depleted in silica and alumina, and the high magnesium andesite/calc-alkaline melts are enriched in silica and alumina. If the interpretation of basanite from the Timanfaya eruption differentiating from subalkaline basalt is correct, then table 4 illustrates a chemical change from a subalkaline melt to an alkaline melt, and this change consists of the depletion in silica and alumina and the increase in all the other major oxides. This is interesting because the change could then be related to electric currents in the magma, given that if a particular magma receives ions transported by induced currents, then the magma would receive network modifying cations that are more mobile, and could shift composition towards more alkaline, silica and alumina depleted, magmas, like alkali basalts, basanites, or melilitites, the opposite may happen in areas that are depleted in network modifying cations, such as Ca or Fe, giving rise to high-magnesium andesites/calc-alkaline magmas that are found in subduction zones.

The first advantage to this idea is that it could explain cases like Timanfaya, Rangitoto, or Udo that were discussed earlier, where a magma like basanite or alkali basalt precedes the eruption of subalkaline basalt, erupting first a differentiated melt that has accumulated network modifying cations and then the original subalkaline melt that hasn't yet been enriched. The second advantage is that it would explain the widespread occurrence of alkaline magmatism in intraplate environments since it would allow the generation of exotic melts from typical mantle composition. Third is that it could explain the opposing aspects of alkaline and high-magnesium andesite/calc-alkaline melts, as displacement of a chemical fraction from one to the other, presumably a displacement of network modifying cations from the latter to the former. There is however the aspect that both are enriched in sodium and potassium oxides relative to the partial melting of peridotite, but this could be explained by both magma types occurring within a wider system that includes for example the

global oceans, a vast storage of various ions that could perhaps be electrically connected to the asthenosphere.

There are some problems to be solved. The first would be the role played by CO2, since as discussed in section 5 carbonated peridotite yields melts that have important similarities to those of alkaline composition. I do think the alkaline melts arise from the differentiation of subalkaline melts and that if there's a role to play it's in the chemical transformation and not generation, but of course, until this is solved it's a problem. Second is that if network-modifying cations are the most mobile and tend to accumulate where alkaline magmas are present then a positive charge will build up in alkaline melts and something must balance this, this would need to be clarified.

The last problem is the mechanism of how and where the network-forming cations accumulate, this could have to do with various aspects such as gradients in volatile contents, temperature, or the geometry of conduits and other magmatic structures in the Earth's interior. Perhaps certain magma geometric structures act as traps for the moving ions. I do think water content is likely to be influential since the silica-enriched, FeO and CaO-depleted, magmas are found in subduction zones where water-rich oceanic material is present. In this context, it would be good to know if gradients in conductivity may favor the migration of moving ions towards areas of lower conductivity during induced currents, given that water can elevate conductivity by an order of magnitude in basaltic melt (Zhang et al., 2021). Temperature will also affect conductivity since it affects polymerization, so if this conductivity gradient does direct the flow of mobile ions it would make sense for them to become enriched in stale intraplate storage and favor highly extremely alkaline magmas in low-activity volcanic fields, like in the Urach case that was described earlier, where low-temperature dry magma may be stored. But of course, this is highly speculative and needs to be clarified by proper mathematical models, experiments, or more data for the idea of induced currents enriching subalkaline magmas with network modifying cations to be established.

6.3 Earth-driven cycles modulate the occurrence of induced currents in the planet.

In section 4, I discussed decadal variations in different phenomena like hailstorms, hurricanes, and various types of volcanism that would be partly powered by electromagnetic induction. Some of these processes showed interesting cycles and/or variations seemingly independent of solar activity, but also seemingly interrelated, and links between geosphere and atmosphere phenomena are most likely to be related to the solar wind connection. This is not surprising since, even under the same solar wind conditions, the Earth would have a different response under different internal conditions, like for example with changes in the conductivity of its components or changes in its magnetic field. So since the Sun is not the only variable that could affect the process of electromagnetic induction in the Earth, it is reasonable to attribute changes in the generation of induction currents and their consequent effects to the other variables: most obviously as a function of changes in the Earth's magnetosphere or the conductivity of the components making up the planet.

Among the conclusions in section 4 was that there was possibly a 50-year periodicity in intraplate alkaline volcanism, given that peaks in such activity took place in 1962, 1906, 1952, and 2003, showing some periodic behavior within the planet, and that these peaks coincided with or ended peaks in hail and hurricane activity. Another conclusion was that hail activity in Spain was inversely correlated with the intraplate subalkaline volcanism of Hawaii, almost as if the oceans and the asthenosphere were competing over the same energy source. Two reductions in Spanish hail activity and an increase in Hawaii intraplate subalkaline volcanism took place around the 1906 and 1952 pulses in alkaline volcanism. All of these changes should be internal Earth processes, given disconnection from sunspot data. As mentioned earlier, perhaps these changes could be viewed as a function of the Earth's magnetosphere or conductivity within the Earth.

When it comes to an explanation regarding these cycles, there could be many, but I think a viable option is for changes in the asthenosphere conductivity to be responsible. The asthenosphere electrical conductivity could be very sensible to changes such as the melting degree (related to temperature), as well as the ionic concentration in the melt. These factors could also potentially have feedback between them. Stronger induced currents will have a greater reduction in the strength of the magnetic field changes within and around the asthenosphere, and if this reduction is of a large enough magnitude it seems viable that it could reduce the induced currents in overlying oceans. Thus shifting induced currents between the hydrosphere and the asthenosphere.

I don't know strong evidence pointing at the specific mechanisms that cause the 50-year periodicity or the likely inverse relationship between induced currents in the asthenosphere and the oceans. So this is a problem to be

solved, perhaps with more data and models regarding changes in the magnetic field, by studying asthenosphere electrical conductivity, or the speed seismic waves passing through this layer, to try and figure out any spatiotemporal changes in these parameters.

7. Summary

This work shows evidence supporting a connection between solar wind conditions in the near-Earth environment and volcanism and weather on Earth. On daily timescales, certain parameters of Kilauea volcano activity related to magma influx respond to changes in the Bx component of the interplanetary magnetic field. On yearly timescales, magma production in several intraplate volcanoes correlates positively with various solar wind parameters, such as solar wind dynamic pressure. A similar pattern can be seen in ≥400 g Spanish hail, where it shows a correlation with the 11-year cycles in solar activity, peaking at the time of the cycle when the interplanetary magnetic field is at its strongest and solar wind dynamic pressure reaches a peak, the match with solar wind dynamic pressure being somewhat poorer, given that hail decays more quickly towards the end of the cycle than this last parameter. These observations support that a paradigm change is needed to better explain the link between solar wind and the atmosphere and geosphere of our planet. An idea is proposed by which deformation of the Earth's magnetosphere by solar wind combined with the planet's rotation exposes locations in the planet to a changing magnetic field and electromagnetic induction of currents in ionic conductors like seawater and magma, which disperse heat, thereby influencing related processes in the atmosphere and geosphere. I also propose these electrical currents may be responsible for the redistribution of certain chemical components within the magma that act as charge carriers, leading to the formation of alkaline, and high magnesium andesite/calc-alkaline melts by the enrichment and depletion respectively of these carriers. All these ideas still need the support of mathematical models, as well as additional data, given that the implications of this process would be very wide yet this article only deals with a local history of hail events and a particular sample of volcanoes.

This article also describes roughly 50-year oscillations that match across different variables, such as North Atlantic hurricane activity, ≥400 g Spanish hail, or intraplate alkaline volcanism. Peaks in activity that seem coincident across the variables, do not appear to correlate with sunspot number, which represents the longest-running record of solar activity and therefore solar wind activity. Instead, I propose these oscillations are internally driven by terrestrial factors influencing the generation of induced currents. However, the exact mechanism would still be lacking.

8. References

Alibert, C., Michard, A., & Albarède, F. (1983). The transition from alkali basalts to kimberlites: Isotope and trace element evidence from melilitites. Contributions to Mineralogy and Petrology, 82(2–3), 176–186. https://doi.org/10.1007/bf01166612

Arai, Y. (2019). History of the development of telecommunications infrastructure in Japan. NETCOM, 33-3/4. https://doi.org/10.4000/netcom.4511

Atlantic hurricane season. (2024, July 2). In Wikipedia. https://en.wikipedia.org/wiki/Atlantic_hurricane_season

Bagnardi, M., & Amelung, F. (2012). Space-geodetic evidence for multiple magma reservoirs and subvolcanic lateral intrusions at Fernandina volcano, Galápagos Islands. Journal of Geophysical Research: Solid Earth, 117(B10). https://doi.org/10.1029/2012jb009465

Best, M.E. (2015). Electromagnetic (EM) Methods; in Shear Wave Velocity Measurement Guidelines for Canadian Seismic Site Characterization in Soil and Rock, (ed.) J.A. Hunter and H.L. Crow; Geological Survey of Canada, Earth Science Sector, General Information Product 110 e, p. 170-180.

Blewitt, G., W. C. Hammond, and C. Kreemer (2018), Harnessing the GPS data explosion for interdisciplinary science, Eos, 99, https://doi.org/10.1029/2018EO104623

Bowen, N. L. (1956). The evolution of the igneous rocks. http://ci.nii.ac.jp/ncid/BA02419894

Brenna, M., Cronin, S. J., Smith, I. E. M., Sohn, Y. K., & Németh, K. (2010). Mechanisms driving polymagmatic activity at a monogenetic volcano, Udo, Jeju Island, South Korea. Contributions to Mineralogy and Petrology, 160(6), 931–950. https://doi.org/10.1007/s00410-010-0515-1

Brenna, M., Ubide, T., Nichols, A. R. L., Mollo, S., and Pontesilli, A. (2021). "Anatomy of Intraplate Monogenetic Alkaline Basaltic Magmatism," in Crustal Magmatic System Evolution: Anatomy, Architecture, and Physico-Chemical Processes. AGU Geophysical Monograph. Editors M. Masotta, C. Beier, and S. Mollo, 264, 79–103. https://doi.org/10.1002/9781119564485.ch4

Bullard, E. C. (1967). Electromagnetic induction in the Earth. Quarterly Journal of the Royal Astronomical Society, 8, 143.

Carracedo J. C., Rodriguez, E., & Soler, V. (1990). Aspectos volcanológicos y estructurales. Evolución petrológica e implicaciones en riesgo volcánico de la erupción de 1730 en Lanzarote. Islas Canarias. Estudios GeolóGicos, 46(1–2). https://doi.org/10.3989/egeol.90461-2436

Conesa, A., 2006. Tormentas severas en la ibérica de Teruel y sus efectos sobre la masa forestal. http://www.divulgameteo.es/uploads/Tormentas-severas-ib%C3%a9rica.pdf

Dasgupta, R., Hirschmann, M. M., & Smith, N. D. (2007). Partial melting experiments of peridotite + CO2 at 3 GPA and genesis of alkalic ocean island basalts. Journal of Petrology, 48(11), 2093–2124. https://doi.org/10.1093/petrology/egm053

D. de B (1828, October 1). Meteroro horroroso. Diario de Zaragoza, p. 3. Retrieved from https://www.zaragoza.es/hemeroteca/prensa/HMZ_P0007/HMZ_P0007_1828-10-01/HMZ_P0007_1828-10-01.pdf

Dickson, A. G., Goyet, C. & DOE. (1994). Handbook of methods for the analysis of the various parameters of the carbon dioxide system in sea water; version 2.

Global Volcanism Program, 2024a. [Database] Volcanoes of the World (v. 5.2.0; 6 Jun 2024). Distributed by Smithsonian Institution, compiled by Venzke, E. https://doi.org/10.5479/si.GVP.VOTW5-2024.5.2

Global Volcanism Program, 2024b. Karthala (233010) in [Database] Volcanoes of the World (v. 5.2.0; 6 Jun 2024). Distributed by Smithsonian Institution, compiled by Venzke, E. https://doi.org/10.5479/si.GVP.VOTW5-2024.5.2

Global Volcanism Program, 2024c. Manam (251020) in [Database] Volcanoes of the World (v. 5.2.0; 6 Jun 2024). Distributed by Smithsonian Institution, compiled by Venzke, E. https://doi.org/10.5479/si.GVP.VOTW5-2024.5.2

Bethencourt, J.., Dorta, P., & Criado, C. (2008). El Temporal de 1826: Reconstrucción de sus causas y sus consecuencias en la isla de Tenerife. In Sigró Rodríguez, J.; Brunet India, M.; Aguilar Anfrons, E. (2008): "Cambio Climático Regional y sus Impactos". Actas del VI Congreso Internacional de Tarragona de la Asociación Española de Climatología (AEC), 8-11 de octubre de 2008.

Hegner, E., Walter, H. J., & Satir, M. (1995). Pb-Sr-Nd isotopic compositions and trace element geochemistry of megacrysts and melilitites from the Tertiary Urach volcanic field: source composition of small volume melts under SW Germany. Contributions to Mineralogy and Petrology, 122(3), 322–335. https://doi.org/10.1007/s004100050131

Hirose, K. (1997). Partial melt compositions of carbonated peridotite at 3 GPa and role of CO2 in alkali-basalt magma generation. Geophysical Research Letters, 24(22), 2837–2840.

Hua, J., Fischer, K. M., Becker, T. W., Gazel, E., & Hirth, G. (2023). Asthenospheric low-velocity zone consistent with globally prevalent partial melting. Nature Geoscience, 16(2), 175–181. https://doi.org/10.1038/s41561-022-01116-9

Japan Meteorological Agency (2013). National catalogue of the active volcanoes in Japan (4th edition). Japan Meteorological Agency. https://www.data.jma.go.jp/vois/data/tokyo/STOCK/souran_eng/souran.htm

King, J. H., & Papitashvili, N. E. (2005). Solar wind spatial scales in and comparisons of hourly wind and Ace Plasma and magnetic field data. Journal of Geophysical Research: Space Physics, 110(A2). https://doi.org/10.1029/2004ja0106492

Kislyakova, K., & Noack, L. (2020). Electromagnetic induction heating as a driver of volcanic activity on massive rocky planets. Astronomy and Astrophysics, 636, L10. https://doi.org/10.1051/0004-6361/202037924

LaFemina, Peter; Amelung, Falk; Geist, Dennis; Chadwick, Bill W.; Meertens, Charles, 2002, Galapagos GPS Network - GV01-GV01 P.S., UNAVCO, GPS/GNSS Observations Dataset, https://doi.org/10.7283/ESJY-V915

Landsea, C. W., and J. L. Franklin, 2013: Atlantic hurricane database uncertainty and presentation of a new database format. Mon. Wea. Rev., 141, 3576–3592, https://doi.org/10.1175/MWR-D-12-00254.1.

Li, L. Y., Zhou, S. P., Wei, S. H., Yang, J. Y., Sauvaud, J. A., & Berthelier, J. J. (2020). The Day-Night difference and geomagnetic activity variation of energetic electron fluxes in region of South Atlantic anomaly. Space Weather, 18(9). https://doi.org/10.1029/2020sw002479

Lockwood, J. P., & Lipman, P. W. (1987). Holocene eruptive history of Mauna Loa volcano. In R. W. Decker, T. L. Wright, & P. H. Stauffer (Eds.), Volcanism in Hawaii (Vol. 1, pp. 509–535). essay, U.S. Geological Survey Professional Paper.H

Longpré, M. A. & Felpeto, A. Historical volcanism in the Canary Islands; part 1: a review of precursory and eruptive activity, eruption parameter estimates, and implications for hazard assessment. J. Volcanol. Geotherm. Res. 419, 107363 (2021).

Lundgren, P., Poland, M., Miklius, A., Orr, T., Yun, S., Fielding, E., Liu, Z., Tanaka, A., Szeliga, W., Hensley, S., & Owen, S. (2013). Evolution of dike opening during the March 2011 Kamoamoa fissure eruption, Kīlauea Volcano, Hawai`i. Journal of Geophysical Research. Solid Earth, 118(3), 897–914. https://doi.org/10.1002/jgrb.50108

Lynn, K. J., Garcia, M. O., Shea, T., Costa, F., & Swanson, D. A. (2017). Timescales of mixing and storage for Keanakāko'i Tephra magmas (1500–1820 C.E.), Kīlauea Volcano, Hawai'i. Contributions to Mineralogy and Petrology, 172(9). https://doi.org/10.1007/s00410-017-1395-4

Matoza, R. S., Shearer, P. M., & Okubo, P. G. (2014). High-precision relocation of long-period events beneath the summit region of Kīlauea Volcano, Hawai'i, from 1986 to 2009. Geophysical Research Letters, 41(10), 3413–3421. https://doi.org/10.1002/2014gl059819

Miklius, Asta, 2000, Hawaii GPS Network - MOKP-Moku`aweoweo P.S., UNAVCO, GPS/GNSS Observations Dataset, https://doi.org/10.7283/T5TQ5ZS9

Miyashiro, A. (1974). Volcanic rock series in island arcs and active continental margins. American Journal of Science, 274(4), 321–355. https://doi.org/10.2475/ajs.274.4.321

Montgomery-Brown, E.K., Sinnett, D.K., Poland, M., Segall, P., Orr, T., Zebker, H., and Miklius, A., 2010. Geodetic evidence for en echelon dike emplacement and concurrent slow slip during the June 2007 intrusion and eruption at Kīlauea volcano, Hawaii: Journal of Geophysical Research, v. 115, no. B7, https://doi.org/10.1029/2009JB006658.

Moragues, G. (1835, September 21). Cronica de las provincia. La Abeja (Madird), p. 2. Retrieved from https://hemerotecadigital.bne.es/hd/es/viewer?id=9814d286-3765-4c64-9290-0982a9ff4bdc&page=2

Needham, A., Lindsay, J., Smith, I., Augustinus, P., & Shane, P. (2011). Sequential eruption of alkaline and sub-alkaline magmas from a small monogenetic volcano in the Auckland Volcanic Field, New Zealand. Journal of Volcanology and Geothermal Research, 201(1–4), 126–142. https://doi.org/10.1016/j.jvolgeores.2010.07.017

Ni, H., Hui, H., & Steinle-Neumann, G. (2015). Transport properties of silicate melts. Reviews of Geophysics, 53(3), 715–744. https://doi.org/10.1002/2015rg000485

Okubo, P. G., & Wolfe, C. J. (2008). Swarms of similar long-period earthquakes in the mantle beneath Mauna Loa Volcano. Journal of Volcanology and Geothermal Research, 178(4), 787–794. https://doi.org/10.1016/j.jvolgeores.2008.09.007

Orr, T. R., Llewellin, E. W., & Patrick, M. R. (2022). Development, structure, and behavior of a perched lava channel at Kīlauea Volcano, Hawai'i, during 2007. Journal of Volcanology and Geothermal Research, 430, 107637. https://doi.org/10.1016/j.jvolgeores.2022.107637

Poland, M. P., Miklius, A., Jeff Sutton, A., & Thornber, C. R. (2012). A mantle-driven surge in magma supply to Kīlauea Volcano during 2003–2007. Nature Geoscience, 5(4), 295–300. https://doi.org/10.1038/ngeo1426

Quien debe pagar los vidrios rotos. (1899, June 13).El Defensor de Granada, p. 2. Retrieved from https://www.bibliotecadigitaldeandalucia.es/

Segall, Paul, Miklius, Asta, 1999, Hawaii GPS Network - AHUP-Ahua P.S., UNAVCO, GPS/GNSS Observations Dataset, https://doi.org/10.7283/T5ST7MW0

Sherrod, D. R., Sinton, J. M., Watkins, S. E., & Brunt, K. M. (2021). Geologic map of the State of Hawaii. Scientific Investigations Map. https://doi.org/10.3133/sim3143

SILSO, World Data Center - Sunspot Number and Long-term Solar Observations, Royal Observatory of Belgium, on-line Sunspot Number catalogue: http://www.sidc.be/SILSO/

Slater, L., Jull, M., McKenzie, D., & Gronvöld, K. (1998). Deglaciation effects on mantle melting under Iceland: results from the northern volcanic zone. Earth and Planetary Science Letters, 164(1–2), 151–164. https://doi.org/10.1016/s0012-821x(98)00200-3

Tyler, R. H., Boyer, T. P., Minami, T., Zweng, M. M., & Reagan, J. R. (2017). Electrical conductivity of the global ocean. Earth Planets and Space, 69(1). https://doi.org/10.1186/s40623-017-0739-7

UNAVCO Community, Smith, Robert B., 2001, Yellowstone Caldera GPS Network - WLWY-White Lake P.S., UNAVCO, GPS/GNSS Observations Dataset, https://doi.org/10.7283/T5765CPG

USGS Hawaiian Volcano Observatory (HVO). (1956). Hawaiian Volcano Observatory Network [Data set]. International Federation of Digital Seismograph Networks. https://doi.org/10.7914/SN/HV

Vinós, J. (2024, May 22). Cómo sabemos que el sol cambia el clima (2). Rankia. https://www.rankia.com/blog/game-over/6380913-como-sabemos-que-sol-cambia-clima-2

Vlastélic, I., Di Muro, A., Bachèlery, P., Gurioli, L., Auclair, D., & Gannoun, A. (2018). Control of source fertility on the eruptive activity of Piton de la Fournaise Volcano, La réunion. Scientific Reports, 8(1). https://doi.org/10.1038/s41598-018-32809-0

Wood, B. J., & Turner, S. P. (2009). Origin of primitive high-Mg andesite: Constraints from natural examples and experiments. Earth and Planetary Science Letters, 283(1–4), 59–66. https://doi.org/10.1016/j.epsl.2009.03.032

Wright, T. L., & Klein, F. W. (2014). Two hundred years of magma transport and storage at Kīlauea Volcano, hawai'i, 1790-2008. Professional Paper. https://doi.org/10.3133/pp1806

Xiang, N. B., Ning, Z. J., & Li, F. Y. (2020). Temporal evolution of the rotation of the interplanetary magnetic field Bx, By, and Bz components. The Astrophysical Journal, 896(1), 12. https://doi.org/10.3847/1538-4357/ab91bc

Yamasato, H. (2005). Modern history of volcano observation in Japan : especially volcano surveillance of Japan Meteorological Agency. Kazan/Kazan. Dai2shu, 50. https://ci.nii.ac.jp/naid/110004702868

Yogodzinski, G. M., Volynets, O. N., Koloskov, A. V., Seliverstov, N. I., & Matvenkov, V. V. (1994). Magnesian andesites and the subduction component in a strongly Calc-Alkaline series at PIIP Volcano, Far Western Aleutians. Journal of Petrology, 35(1), 163–204. https://doi.org/10.1093/petrology/35.1.163

Yu, J., Li, L., Cao, J. B., Reeves, G. D., Baker, D. N., & Spence, H. (2016). The influences of solar wind pressure and interplanetary magnetic field on global magnetic field and outer radiation belt electrons. Geophysical Research Letters, 43(14), 7319–7327. https://doi.org/10.1002/2016gl069029

Wasylenki, L. E. (2003). Near-solidus melting of the shallow upper mantle: partial melting experiments on depleted peridotite. Journal of Petrology, 44(7), 1163–1191. https://doi.org/10.1093/petrology/44.7.1163

Wilson, M., Rosenbaum, J. M., & Dunworth, E. A. (1995). Melilitites: partial melts of the thermal boundary layer? Contributions to Mineralogy and Petrology, 119(2–3), 181–196. https://doi.org/10.1007/bf00307280

Zhang, B.H.; Guo, X.; Yoshino, T.; Xia, Q.K. (2021). Electrical conductivity of melts: Implications for conductivity anomalies in the Earth's mantle. Natl. Sci. Rev., 8(11). https://doi.org/10.1093/nsr/nwab064

9. Appendix

The following table lists Spanish hail events with stones equaling or exceeding 400 grams weight since 1850 documented in newspapers. Each row represents a different storm and data is displayed for the location of the heaviest reported hail. Sources and links are given, additional data regarding damage, hour of the event, or other details can be found in the newspaper sources. Data is particularly incomplete during the Third Carlist War (1872-1876), and fully missing during the Civil War (1936-1939) and probably incomplete during the following years of recovery from the conflict. Presential means the newspapers are not freely accessible online,

only in the library itself. A pound is assumed to weigh 460 g, and an ounce 28.75 g (which should be the Spanish mass standards).

Location (province)	dd/mm/yyyy	Grams	Newspaper (publication city). Date. Database. Link.	Notes
Maluenda (Zaragoza)	18/7/2006	400	El Periódico de Aragón 5/8/2006. Hemeroteca Digital BNE (presential).	
Chiclana de Segura (Jaén)	15/6/2006	1300	El Ideal (Jaén). 17/6/2006. Hemeroteca Digital BNE (presential).	May be incorrect since the same report mentions stones to have 7 cm diameter.
Alcañiz (Teruel)	16/8/2003	900	Webpage: Jose A. Quirantes. Descomunal Granizada y posible Supercélula HP (High Precipitation) Alcañiz (Teruel), 16 agosto-2003. http://www.tiemposevero.es/ver-reportaje.php?id=36	Large hailstones weighed 500 g, and very few 900 g.
Alfafara (Alicante)	25/7/1986	600	La Vanguardia (Barcelona). 28/7/1986. Hemeroteca Digital BNE (presential).	Additional reports of 12-cm-diameter hail in Agullent “Diario de Ibiza. 27/7/1986”, and 18-cm-diameter hail in Valle de Albaida “Diario de León. 28/7/1986”.
Navás (Barcelona)	4/7/1984	400	La Vanguardia (Barcelona). 9/7/1984. Hemeroteca Digital BNE (presential).	
Tobarra (Albacete)	19/9/1982	400	Línea (Murcia). 24/9/1982. Archivo Municipal de Murcia. https://www.archivodemurcia.es/p_pandora4/viewer.vm?id=0000592620&page=13&lang=es&view=hemeroteca	350-400 g in weight
Zuera (Zaragoza)	23/8/1982	400	Aragón Expres (Zaragoza). 26/08/1982. Biblioteca Virtual de Prensa Histórica. https://prensahistorica.mcu.es/es/catalogo_imagenes/grupo.do?path=185075&idBusqueda=9522&presentacion=pagina&posicion=15	
Yecla (Murcia)	18/8/1976	400	Línea (Murcia), 20/8/1976. Archivo Municipal de Murcia. https://www.archivodemurcia.es/p_pandora4/viewer.vm?id=0000520636&page=10&view=hemeroteca	
Úbeda (Jaen)	14/8/1975	400	El Ideal (Jaén). 16/08/1975. Hemeroteca Digital BNE (presential).	
El Burgo de Ebro (Zaragoza)	29/8/1974	400	Aragón Expres (Zaragoza). 30/8/1974. Biblioteca Virtual de Prensa Histórica. https://prensahistorica.mcu.es/es/catalogo_imagenes/grupo.do?path=2001122362&idBusqueda=9333&posicion=12&presentacion=pagina	
Chinchilla (Albacete)	20/9/1962	500	Línea (Murcia) 21/9/1962. Archivo Municipal de Murcia. https://www.archivodemurcia.es/p_pandora4/viewer.vm?id=0000402071&page=5&view=hemeroteca	Chinchilla or nearby towns
Zona de Sort (Lérida)	?/7/1962	600	Hoja Oficial del Lunes (Madrid). 30/7/1962. Biblioteca Virtual de Prensa Histórica. https://prensahistorica.mcu.es/es/catalogo_imagenes/grupo.do?path=7150055&idImagen=70812626&idBusqueda=9029&posicion=1&presentacion=pagina	
Vich (Barcelona)	26/7/1960	650	La Rioja (Logroño) 27/7/1960. Biblioteca Virtual de Prensa Histórica. https://prensahistorica.mcu.es/es/catalogo_imagenes/grupo.do?path=297638&idImagen=2010224705&idBusqueda=8960&posicion=8&presentacion=pagina	
Alcorlo, (Guadalajara)	24/9/1959	470	Nueva Alcarria (Guadalajara). 3/10/ 1959. Biblioteca Virtual de Prensa Histórica. https://prensahistorica.mcu.es/es/catalogo_imagenes/grupo.do?path=5083943&idImagen=50521454&idBusqueda=8915&posicion=2&presentacion=pagina	Day not exactly known
Fuenterrobles (Valencia)	17/9/1958	500	Diario de Burgos (Burgos). 18/9/1958. Biblioteca Virtual de Prensa Histórica. https://prensahistorica.mcu.es/es/catalogo_imagenes/grupo.do?path=1000454439&idImagen=1003347344&idBusqueda=8700&posicion=4&presentacion=pagina	
Irijo (Orense)	27/7/1955	500	El Diario de Ávila (Ávila). 28/07/1955. Biblioteca Virtual de Prensa Histórica. https://prensahistorica.mcu.es/es/catalogo_imagenes/grupo.do?path=675108&posicion=3&presentacion=pagina	From 100 to 500 g in weight. Location approximate.
Madridejos (Toledo)	28/8/1952	1000	Informaciones (Madrid). 29/8/1952. Hemeroteca Digital BNE (presential).	0.5 kg and up to 1 kg
Es Llombars (Baleares)	17/8/1952	1500	La Almudaina (Palma de Mallorca). 19/8/1952. Biblioteca Virtual de Prensa Histórica. https://prensahistorica.mcu.es/es/catalogo_imagenes/grupo.do?path=179369&posicion=2&presentacion=pagina	Hailstone made a hole in the roof of the Es Llombars church so big as to allow a man through, it was recovered and weighed in 1.5 kg. Independent report of 1.5 kg hail exists from Campos area in "Baleares (Palma de Mallorca) 20/8/1952".
Pedrajas de San Esteban (Valladolid)	1/7/1952	400	El Adelantado (Segovia). 2/7/1952. Biblioteca Virtual de Prensa Histórica. https://prensahistorica.mcu.es/es/catalogo_imagenes/grupo.do?path=599656&posicion=1&presentacion=pagina	
Castejón de Monegros (Huesca)	11/6/1950	750	Nueva España (Huesca). 13/6/1950. Hemeroteca Diario del Alto Aragón. https://hemeroteca.diariodelaltoaragon.es	
Cartagena (Murcia)	11/9/1949	1500	El Noticiero de Cartagena (Cartagena). 13/9/1949. Archivo Municipal de Cartagena. https://archivo.cartagena.es/pandora/cgi-bin/Pandora.exe?xslt=ejemplar;publication=El%20Noticiero;day=13;month=09;year=1949;page=001;id=0000124183;collection=pages;url_high=pages/El%20Noticiero/1949/194909/19490913/El%20Noticiero%2019490913-001.pdf;lang=es;encoding=utf-8	Two witnesses to the weight measurement of a 1500 g hailstone collected from Plaza de España inform the newspaper. Another measurement of 1073 g hail is reported by the same news a day earlier. Hailstones blew straight through the clay roofs of many buildings in the city center “La Verdad de Murcia. 13/9/1949”
Torrevieja (Alicante)	11/9/1949	400	La Verdad de Murcia (Murcia). 14/9/1949. Archivo Municipal de Murcia. https://www.archivodemurcia.es/p_pandora4/viewer.vm?id=0000810335&page=3&view=hemeroteca	Despite proximity to Cartagena hailstorm, the hours earlier occurrence means it was a different storm.

Villafranca de los Caballeros (Toledo)	6/9/1949	1000	Guadalajara (Guadalajara). 8/9/1949. Biblioteca Virtual de Prensa Histórica. https://prensahistorica.mcu.es/es/catalogo_imagenes/grupo.do?path=4018004&posicion=1&presentacion=pagina	Some stones were over 1 kg in weight and had the size and shape of paving stones (~20 cm length and elongated). Independent report of 750 g hail exists from Alcázar in "Lanza (Ciudad Real) 8/9/1949" that broke a person's arm.
Puente de Vallecas (Madrid)	5/9/1949	700	Madrid (Madrid). 6/9/1949. Hemeroteca Digital BNE (presential).	Hail blew through roof of a house shattering objects inside room "El Noticiero (Zaragoza). 6/9/1949".
Siguenza (Guadalajara)	5/9/1949	500	Nueva Alcarria (Guadalajara). 10/9/1949. Biblioteca Virtual de Prensa Histórica. https://prensahistorica.mcu.es/es/catalogo_imagenes/grupo.do?path=5084390&posicion=1&presentacion=pagina	Closely related to Madrid storm, but likely different cell, too much distance and too close in time for Madrid storm to have moved to Siguenza in time.
Alberite (La Rioja)	26/8/1949	1000	La Rioja (Logroño). 28/8/1949. Biblioteca Virtual de Prensa Histórica. https://prensahistorica.mcu.es/es/catalogo_imagenes/grupo.do?path=254500&presentacion=pagina&idBusqueda=7894&posicion=5	Some 700 g, and a block of more than 1 kg
Encinacorba (Zaragoza)	9/6/1949	500	El Noticiero (Zaragoza). 15/6/1949. Hemeroteca del Ayuntamiento de Zaragoza. https://www.zaragoza.es/hemeroteca/prensa/HMZ_P0016/HMZ_P0016_1949-06-15/HMZ_P0016_1949-06-15.pdf	More than half a kg
Calahorra (La Rioja)	17/8/1948	400	La Rioja (Logroño). 18/8/1948. Biblioteca Virtual de Prensa Histórica. https://prensahistorica.mcu.es/es/catalogo_imagenes/grupo.do?path=254181&idImagen=2010007356&idBusqueda=7719&posicion=4&presentacion=pagina	
Tudela (Navarra)	16/8/1948	1500	Diario de Navarra (Pamplona). 18 de agosto de 1948. Hemeroteca Digital BNE (presential).	First-hand statement of the person who weighed a 1500 g hailstone, who also added that other stones reached 900 g, and most had 300 g.
Oteiza de la Solana (Navarra)	1/8/1948	500	El adelantado (Segovia). 6/8/1948. Biblioteca Virtual de Prensa Histórica. https://prensahistorica.mcu.es/es/catalogo_imagenes/grupo.do?path=598454&idImagen=2011968315&idBusqueda=7761&posicion=3&presentacion=pagina	Half a kg
Ariza (Zaragoza)	30/7/1948	500	El adelantado (Segovia). 31/7/1948. Biblioteca Virtual de Prensa Histórica. https://prensahistorica.mcu.es/es/catalogo_imagenes/grupo.do?path=598449&idImagen=2011968294&idBusqueda=7276&posicion=4&presentacion=pagina	In the area of Alhama, Ariza and Cetina. Exact day unknown.
Cazorla (Jaen)	3/9/1947	745	Libertad (Valladolid). 04/09/1947. Biblioteca Virtual de Prensa Histórica. https://prensahistorica.mcu.es/es/catalogo_imagenes/grupo.do?path=274428&idImagen=2010093843&idBusqueda=7215&posicion=1&presentacion=pagina	250 g in Cazorla itself. 516 g and up to 745 g in the countryside. Year of the newspaper dubbed incorrectly in the digital library. Exact day not known.
Cadrete (Zaragoza)	13/6/1947	500	Pueblo (Madrid). 14/06/1947. Biblioteca Virtual de Prensa Histórica. https://prensahistorica.mcu.es/es/catalogo_imagenes/grupo.do?path=234810&idImagen=2009939304&idBusqueda=7155&posicion=3&presentacion=pagina	Half a kg. Cadrete and Maria de Huerva
Ontur (Albacete)	30/6/1945	940	El Diario de Ávila (Avila). 5/7/1945. Biblioteca Virtual de Prensa Histórica. https://prensahistorica.mcu.es/es/catalogo_imagenes/grupo.do?path=672104&idImagen=2012260595&idBusqueda=7116&posicion=1&presentacion=pagina	A hailstone reached 940 g. Others weighed 820-770 g. Pierced roofs and metal shutters.
Albudeite (Murcia)	20/6/1944	2000	Línea (Murcia). 23/6/1944. Archivo Municipal de Murcia. https://www.archivodemurcia.es/p_pandora4/viewer.vm?id=0000334583&page=9&view=hemeroteca	Many stones over 0.5 kg, and some close to 2 kg in weight
Daroca (Zaragoza)	3/8/1943	550	Heraldo de Aragón (Zaragoza). 4/8/1943. Hemeroteca del Ayuntamiento de Zaragoza. https://www.zaragoza.es/hemeroteca/prensa/HMZ_P0178/HMZ_P0178_1943-08-04/HMZ_P0178_1943-08-04.pdf	
El Poyo (Pontevedra)	28/1/1941	600	El Adelantado (Segovia). 28/1/1941. Biblioteca Virtual de Prensa Histórica. https://prensahistorica.mcu.es/es/catalogo_imagenes/grupo.do?path=596135&idImagen=2011958891&idBusqueda=10749&posicion=2&presentacion=pagina	
Castejón (Navarra)	7/7/1936	500	La Rioja (Logroño) 10/07/1936. Biblioteca Virtual de Prensa Histórica. https://prensahistorica.mcu.es/es/catalogo_imagenes/grupo.do?path=295425&idImagen=2010209370&idBusqueda=3725&posicion=2&presentacion=pagina	0.5 kg. Days before start of civil war, which leads to complete lack of hail information until 1939, and possibly lessened information for some years afterward.
Pozuel de Ariza (Zaragoza)	13/6/1936	500	Heraldo de Aragón (Zaragoza). 16/6/1936. Hemeroteca del Ayuntamiento de Zaragoza. https://www.zaragoza.es/hemeroteca/prensa/HMZ_P0178/HMZ_P0178_1936-06-16/HMZ_P0178_1936-06-16.pdf	0.5 kg. Location approximate
Carrascal del Obispo (Salamanca)	7/8/1935	400	Ahora (Madrid). 9/8/1935. Hemeroteca Digital BNE. https://hemerotecadigital.bne.es/hd/es/viewer?id=f26feb64-0820-4160-b4a2-0075a9d44c53&page=4	
Figueres (Gerona)	2/8/1934	450	Diari de Girona d'avisos i notícies (Gerona). 3/8/1934. https://pandora.girona.cat/viewer.vm?id=0000572930&page=3&search=tempesta%20pedra%20grams&lang=es&view=hemeroteca	
Santa Eulalia (Teruel)	?/8/1934	400	La Libertad (Madrid). 21/8/1934. https://hemerotecadigital.bne.es/hd/es/viewer?id=cc593c70-73c9-468d-a28a-f67747535a95&page=3	
Godella (Valencia)	12/7/1932	500	El Pueblo (Valencia). 14/7/1932. Biblioteca Virtual de Prensa Histórica. https://prensahistorica.mcu.es/es/catalogo_imagenes/grupo.do?path=1000182239&idImagen=1001260953&idBusqueda=6531&posicion=2&presentacion=pagina	Location approximate
Montilla (Córdoba)	3/9/1929	500	El Guadalete (Jerez de la Frontera). 6/9/1929. Biblioteca Digital Andalucía. https://www.bibliotecadigitaldeandalucia.es/catalogo/es/catalogo_imagenes/grupo.do?path=112658&idImagen=4395961&idBusqueda=1218&posicion=2&presentacion=pagina	
Totana (Murcia)	16/8/1928	500	El Liberal de Murcia (Murcia). 17/8/1928. Archivo Municipal de Murcia. https://www.archivodemurcia.es/p_pandora4/viewer.vm?id=0000306025&page=2	
Cariñena (Zaragoza)	5/9/1927	900	La Voz de Aragón (Zaragoza). 7/9/1927. https://www.zaragoza.es/hemeroteca/prensa/HMZ_P0038/HMZ_P0038_1927-09-07/HMZ_P0038_1927-09-07.pdf	More than 900 g, others had 250-750 g.
Calanda (Teruel)	20/5/1927	485	El Siglo futuro (Madrid). 24/5/1927. Hemeroteca Digital BNE. https://hemerotecadigital.bne.es/hd/es/viewer?id=da5f2e25-c783-4c40-baa7-867e6a4ec747&page=4	

Alquezar (Huesca)	28/7/1924	700	Diario de Huesca (Huesca). 31/07/1924. Hemeroteca Diario del Alto Aragón. https://hemeroteca.diariodelaltoaragon.es	Location approximate.
Jarque (Zaragoza)	16/9/1921	700	Heraldo de Aragón (Zaragoza). 21/9/1921. Hemeroteca del Ayuntamiento de Zaragoza. https://www.zaragoza.es/hemeroteca/prensa/HMZ_P0178/HMZ_P0178_1921-09-21/HMZ_P0178_1921-09-21.pdf	
Antillón (Huesca)	28/8/1915	700	Diario de Huesca (Huesca) 1/9/1915. Hemeroteca Diario del Alto Aragón. https://hemeroteca.diariodelaltoaragon.es	Orange-sized stones blew through the roofs of houses, penetrating rooms. A 700 g stone was weighed in a store.
Urrea de Gaén (Teruel)	26/8/1915	460	Heraldo de Aragón (Zaragoza). 31/8/1915. Hemeroteca del Ayuntamiento de Zaragoza. https://www.zaragoza.es/hemeroteca/prensa/HMZ_P0178/HMZ_P0178_1915-08-31/HMZ_P0178_1915-08-31.pdf	More than a pound
Zuera (Zaragoza)	29/7/1915	600	El Imparcial (Madrid). 1/8/1915. Hemeroteca Digital BNE. https://hemerotecadigital.bne.es/hd/es/viewer?id=43963634-e80e-47be-9c89-d64229381336	Great thickness. Accompanied by a downburst. A few people killed by the hailstones.
Villanueva de Huerva (Zaragoza)	23/6/1915	1400	Heraldo de Aragon (Zaragoza). 25/6/1915. Hemeroteca del Ayuntamiento de Zaragoza. https://www.zaragoza.es/hemeroteca/prensa/HMZ_P0178/HMZ_P0178_1915-06-25/HMZ_P0178_1915-06-25.pdf	3 pounds. Left holes in the ground bigger than two adult fists together. Woman so injured as to stay bedridden.
Mora de Ebro (Tarragona)	17/6/1915	920	La Cruz (Tarragona). 20/6/1915. Biblioteca Virtual de Prensa Histórica. https://prensahistorica.mcu.es/es/catalogo_imagenes/grupo.do?path=3046667&idImagen=30262842&idBusqueda=5742&posicion=2&presentacion=pagina	2 pounds. In García size of oranges. In Mora la Nueva weight is reported to be similar to Mora de Ebro.
Portugalete (Vizcaya)	17/9/1913	400	La Correspondencia de España (Madrid). 19/9/1913. Hemeroteca Digital BNE. https://hemerotecadigital.bne.es/hd/es/viewer?id=1eccedfe-664b-49e8-8303-4916f1d284c9	Location approximate
Alberique (Valencia)	25/7/1913	600	El Diluvio (Barcelona). 27/7/1913. Arxiu de Revistes Catalanes Antigues. https://arca.bnc.cat/arcabib_pro/es/catalogo_imagenes/grupo.do?path=1397770&idImagen=13724800&idBusqueda=9402&posicion=47&presentacion=pagina	Location unclear
Nafría de Úcero (Soria)	13/7/1912	476	El avisador numantino (Soria). 1912 julio 17. Biblioteca Virtual de Prensa Histórica. https://prensahistorica.mcu.es/es/catalogo_imagenes/grupo.do?path=2213652&idImagen=21160898&idBusqueda=5527&posicion=1&presentacion=pagina	
Tallada d'Emporda (Gerona)	22/5/1912	1500	Diari de Girona d'avisos i notícies. 28/5/1912. Arxiu Municipal de Girona. https://pandora.girona.cat/viewer.vm?id=0000535496&page=3	More than 1500 g. Only mentions the death of a cavalry animal. In Tallada or Bellcaire.
Dolores (Alicante)	9/9/1910	450	El Heraldo de Madrid (Madrid). 12/9/1910. Hemeroteca Digital BNE. https://hemerotecadigital.bne.es/hd/es/viewer?id=9ccbd30b-afbd-4fdb-a94a-5be2fcd8388e&page=2	
Sagunto (Valencia)	22/8/1908	400	El Correo español (Madrid). 24/8/1908. Hemeroteca Digital BNE. https://hemerotecadigital.bne.es/hd/es/viewer?id=4f6c5577-f6bc-47a0-a711-57b12c245954&page=3	Exact date unclear
Quintanar de la Orden (Toledo)	28/8/1907	500	La Liga Agraria (Madrid). 10/09/1907. Biblioteca Virtual de Prensa Histórica. https://prensahistorica.mcu.es/es/catalogo_imagenes/grupo.do?path=348463&presentacion=pagina&idBusqueda=5086&posicion=2	
Brea de Tajo (Madrid)	28/8/1907	500	La Liga Agraria (Madrid). 10/09/1907. Biblioteca Virtual de Prensa Histórica. https://prensahistorica.mcu.es/es/catalogo_imagenes/grupo.do?path=348463&presentacion=pagina&idBusqueda=5086&posicion=2	
Callús (Barcelona)	27/7/1906	570	Diario de Huesca (Huesca) 30/07/1906. Hemeroteca Diario del Alto Aragón. https://hemeroteca.diariodelaltoaragon.es	20 ounces. Exact date unclear.
Alcañiz (Teruel)	6/9/1904	400	Diario de Huesca (Huesca) 12/09/1904. Hemeroteca Diario del Alto Aragón. https://hemeroteca.diariodelaltoaragon.es	14 ounces
Agreda (Soria)	6/6/1904	460	Diario de Avisos (Zaragoza) 9/6/1904. Hemeroteca del Ayuntamiento de Zaragoza. https://www.zaragoza.es/hemeroteca/prensa/HMZ_P0015/HMZ_P0015_1904-06-09/HMZ_P0015_1904-06-09.pdf	15-16 ounces
Gallur (Zaragoza)	?/7/1902	400	Diario de Huesca (Huesca). 17/07/1902. Hemeroteca Diario del Alto Aragón. https://hemeroteca.diariodelaltoaragon.es	
Cornago (La Rioja)	?/9/1901	920	Crónica de Vinos y Cereales (Zaragoza). 11/9/1901. Biblioteca Virtual de Prensa Histórica. https://prensahistorica.mcu.es/es/catalogo_imagenes/grupo.do?path=2001025738&idImagen=2008440727&idBusqueda=4816&posicion=3&presentacion=pagina	2 pounds
Pedro Martinez (Granada)	?/6/1901	400	El Universo (Madrid). 23/6/1901. Hemeroteca Digital BNE. https://hemerotecadigital.bne.es/hd/es/viewer?id=2b86ad11-12cd-4915-b968-d939639881af&page=3	14 ounces
Castellote (Teruel)	7/9/1900	430	El Mercantil de Aragón (Zaragoza). 17/9/1900. Hemeroteca del Ayuntamiento de Zaragoza. https://www.zaragoza.es/hemeroteca/prensa/HMZ_P0154/HMZ_P0154_1900-09-17/HMZ_P0154_1900-09-17.pdf	15 ounces
Albelda (Huesca)	7/8/1900	2000	Diari de Girona d'avisos i notícies (Gerona). Arxiu Municipal de Girona. 14/8/1900. https://pandora.girona.cat/viewer.vm?id=0000193657&page=4	Many over 0.5 kg, and up to 2 kg. Person killed by hail.
Navaridas (Álava)	1/8/1898	690	Crónica de Vinos y Cereales (Zaragoza). 10/8/1898. Biblioteca Virtual de Prensa Histórica. https://prensahistorica.mcu.es/es/catalogo_imagenes/grupo.do?path=2001025577&presentacion=pagina&idBusqueda=17175&posicion=3	1.5 pounds
Almansa (Albacete)	29/7/1898	630	La Correspondencia militar (Madrid). 2/8/1898 Hemeroteca Digital BNE. https://hemerotecadigital.bne.es/hd/es/viewer?id=33fc5eb7-65f9-46da-95de-8a7f63d26453&page=2	22 ounces
Campo de Cariñena (Zaragoza)	9/9/1897	430	Crónica de Vinos y Cereales (Zaragoza). 22/9/1897. Biblioteca Virtual de Prensa Histórica. https://prensahistorica.mcu.es/es/catalogo_imagenes/grupo.do?path=2001025531&idImagen=2008439899&idBusqueda=17141&posicion=3&presentacion=pagina	15 ounces. Approximate area. Exact date unclear.
Pego (Valencia)	20/8/1896	500	Heraldo de Baleares (Palma de Mallorca). 23/08/1896. Biblioteca Virtual de Prensa Histórica. https://prensahistorica.mcu.es/es/catalogo_imagenes/grupo.do?path=1132095&idImagen=10604354&idBusqueda=17112&posicion=3&presentacion=pagina	More than 0.5 kg. Exact date unclear. Two children killed by hail.

Caspe (Zaragoza)	18/8/1895	1500	La Rioja (Logroño) 22/08/1895. Biblioteca Virtual de Prensa Histórica. https://prensahistorica.mcu.es/es/catalogo_imagenes/grupo.do?path=3082908&posicion=1&presentacion=pagina	1 kg and 1.5 kg in weight, size and shape like breads.
Alfaro (Navarra)	30/8/1894	400	El Liberal navarro (Pamplona). 31/08/1894. Biblioteca Virtual de Prensa Histórica. https://prensahistorica.mcu.es/es/catalogo_imagenes/grupo.do?path=6010382&idImagen=60209357&idBusqueda=16977&posicion=2&presentacion=pagina	14 ounces. Location approximate.
Villafranca de los Caballeros (Toledo)	12/8/1894	460	La Correspondencia de España (Madrid). 16/8/1894. Hemeroteca Digital BNE. https://hemerotecadigital.bne.es/hd/es/viewer?id=9b0b6832-7400-4ff4-add7-6a4ae0752e90&page=2	Originally perhaps 1 pound report?
Fontanarejo (Ciudad Real)	14/9/1893	1000	El Siglo futuro (Madrid). 22/9/1893. Hemeroteca Digital BNE. https://hemerotecadigital.bne.es/hd/es/viewer?id=0876ae65-bdfa-4456-8bda-8a7048d35b9e	Most weighed 300 grams, some over 1 kg (credible cosidering that pig skulls were "completely smashed" and cows killed). Exact date unclear.
Villanueva de Bogas (Toledo)	14/9/1893	460	Diario de Manila (Manila). 31/10/1893. Hemeroteca Digital BNE. https://hemerotecadigital.bne.es/hd/es/viewer?id=a2413805-0072-416e-b52c-a78214a32a0c&page=3	1 pound
La Ametla (Tarragona)	13/7/1893	400	El Correo de la Provincia (Tarragona). 15/07/1893. Arxiu de l'Ajuntament de Tarragona.	
Villamanrique (Madrid)	21/8/1890	460	El Día (Madrid). 24/8/1890. Hemeroteca Digital BNE. https://hemerotecadigital.bne.es/hd/es/viewer?id=e306f3c6-d34f-4a0f-851a-20decf7d95b1	14-16 ounces
Alloza (Teruel)	28/7/1890	630	Crónica de Vinos y Cereales (Zaragoza). 9/8/1890. Biblioteca Virtual de Prensa Histórica. https://prensahistorica.mcu.es/es/catalogo_imagenes/grupo.do?path=2001025037&idImagen=2008437917&idBusqueda=14957&posicion=2&presentacion=pagina	Most 6-7 ounces in weight. Narrator weighed a 13-ounce stone. Another person a 22-ounce stone. Blew through tiles and woodplanks of a roof.
Gurrea de Gállego (Huesca)	28/7/1890	400	Crónica de Vinos y Cereales (Zaragoza). 6/8/1890. Biblioteca Virtual de Prensa Histórica. https://prensahistorica.mcu.es/es/catalogo_imagenes/grupo.do?path=2001025036&idImagen=2008437914&idBusqueda=16769&posicion=3&presentacion=pagina	
Lluchmayor (Baleares)	27/9/1885	460	Gaceta universal (Madrid). 3/10/1885. Hemeroteca Digital BNE. https://hemerotecadigital.bne.es/hd/es/viewer?id=0f50c732-6c70-42f4-bb69-813d48c3f1f9&page=2	0.5 and more than 1 pound
Ciudadela (Baleares)	26/9/1885	520	El católico (Mahón). 3/10/1885. Biblioteca Virtual de Prensa Histórica. https://prensahistorica.mcu.es/es/catalogo_imagenes/grupo.do?path=3001631&idImagen=30010812&idBusqueda=16613&posicion=8&presentacion=pagina	11, 13, 15, 18 ounces
Igualada (Barcelona)	10/8/1885	460	Crónica de Vinos y Cereales (Zaragoza). 12/08/1885. Biblioteca Virtual de Prensa Histórica. https://prensahistorica.mcu.es/es/catalogo_imagenes/grupo.do?path=2001024622&idImagen=2008436256&idBusqueda=16344&posicion=2&presentacion=pagina	1 pound
Hernani (Guipuzcoa)	1/8/1885	460	La Correspondencia de España (Madrid). 7/8/1885. Biblioteca Virtual de Prensa Histórica. https://prensahistorica.mcu.es/es/catalogo_imagenes/grupo.do?path=6057893&posicion=3&presentacion=pagina	10-16 ounces
Olot (Gerona)	19/8/1884	460	La Unión (Madrid). 23/8/1884. Hemeroteca Digital BNE. https://hemerotecadigital.bne.es/hd/es/viewer?id=d1899336-1ddf-41d5-8087-e63c2bcc5c8d&page=3	10 ounces and up to 1 pound
Talarn (Lerida)	7/8/1884	430	El Imparcial (Madrid). 12/8/1884. Hemeroteca Digital BNE. https://hemerotecadigital.bne.es/hd/es/viewer?id=0e381550-7ac5-46a8-93c2-62f08d17ea8a&page=2	15 ounces
Yeste (Albacete)	8/7/1884	860	El Diario de Albacete (Albacete). 12/7/1935. Biblioteca Digital de Albacete. https://iealbacetenses.dipualba.es/viewer.vm?id=0000017196&page=1&lang=es&view=press	25 and 30 ounces
La Codoñera (Teruel)	8/7/1884	570	Diario de Avisos (Zaragoza). 12/7/1884. Hemeroteca del Ayuntamiento de Zaragoza. https://www.zaragoza.es/hemeroteca/prensa/HMZ_P0015/HMZ_P0015_1884-07-12/HMZ_P0015_1884-07-12.pdf	17 and 21 ounces
La Palma (Murcia)	26/5/1884	460	La Correspondencia de España (Madrid). 28/5/1884. Hemeroteca Digital BNE. https://hemerotecadigital.bne.es/hd/es/viewer?id=56036d74-5c9c-4758-a2b4-42814aebeb11	More than 1 pound.
Castellterçol (Barcelona)	31/8/1881	460	Crónica de Cataluña (Barcelona). 3/9/1881. Hemeroteca Digital BNE. https://hemerotecadigital.bne.es/hd/es/viewer?id=96cbb038-4cb3-458b-ac75-a9a86ce277c4&page=2	1 pound
Albaida (Valencia)	23/8/1881	580	La Discusión (Madrid). 30/8/1881. Hemeroteca Digital BNE. https://hemerotecadigital.bne.es/hd/es/viewer?id=a5b3fb7b-43c4-44a2-a98b-b27a890705ed&page=3	20 ounces
Artá (Baleares)	4/6/1881	430	El Defensor de Granada (Granada). 7/6/1881. Biblioteca Digital de Andalucía. https://www.bibliotecadigitaldeandalucia.es/catalogo/es/catalogo_imagenes/grupo.do?path=168811&idBusqueda=46933&posicion=1	15 ounces. Manacor to Artá.
Requena (Valencia)	22/8/1880	720	Gaceta universal (Madrid). 27/8/1880. Hemeroteca Digital BNE. https://hemerotecadigital.bne.es/hd/es/viewer?id=608d6852-6cdb-4de8-bd0a-b056448eae04&page=2	25 ounces. Exact date unclear.
Gandesa (Tarragona)	21/9/1877	780	Diario de Avisos (Zaragoza). 26/9/1877. Hemeroteca del Ayuntamiento de Zaragoza. https://www.zaragoza.es/hemeroteca/prensa/HMZ_P0015/HMZ_P0015_1877-09-26/HMZ_P0015_1877-09-26.pdf	27 ounces
Hijar (Teruel)	21/8/1876	520	Diario de Avisos (Zaragoza). 30/8/1876. Hemeroteca del Ayuntamiento de Zaragoza. https://www.zaragoza.es/hemeroteca/prensa/HMZ_P0015/HMZ_P0015_1876-08-30/HMZ_P0015_1876-08-30.pdf	18 ounces
Calasparra (Murcia)	10/9/1875	920	La Paz de Murcia (Murcia). 15/9/1875. Archivo Municipal de Murcia. https://www.archivodemurcia.es/p_pandora4/viewer.vm?id=0000651664&page=1&view=hemeroteca	2 pounds. A stone weighed an hour after the storm gave 5 quarters of a pound

Almonacid de la Sierra (Zaragoza)	24/6/1871	780	Crónica de Cataluña (Barcelona). 4/7/1871. Hemeroteca Digital BNE. https://hemerotecadigital.bne.es/hd/es/viewer?id=a1f8a179-5c0d-4c9b-92c6-ca91541b2c4d&page=3	6 to 27 ounces.
Belorado (Burgos)	29/7/1869	1400	La Discusión (Madrid). 5/8/1869. Hemeroteca Digital BNE. https://hemerotecadigital.bne.es/hd/es/viewer?id=6f7b8065-b02b-4a84-87b9-4f0b4ddc5b3d&page=4	2-3 pounds. Most half a pound.
Olván (Barcelona)	16/7/1868	690	El Eco de Aragón (Zaragoza), p. 3. 22/7/1868. Hemeroteca del Ayuntamiento de Zaragoza. https://www.zaragoza.es/hemeroteca/prensa/HMZ_P0159/HMZ_P0159_1868-07-22/HMZ_P0159_1868-07-22.pdf	1.5 pounds
Puebla de Valbona (Valencia)	13/9/1867	460	El Pensamiento español (Madrid). 18/9/1867. Hemeroteca Digital BNE. https://hemerotecadigital.bne.es/hd/es/viewer?id=a1eab426-6eb8-4aca-acb8-263b68eb178c&page=4	Most 2 ounces, and up to 1 pound
Camporobres (Valencia)	14/8/1864	460	El Clamor público (Madrid). 26/8/1864. Hemeroteca Digital BNE. https://hemerotecadigital.bne.es/hd/es/viewer?id=b36e0fee-85c9-45d7-b736-f8e9b608334e&page=2	Many reached 1 pound, most 6-8 ounces
Requesens (Gerona)	31/7/1864	600	El Clamor público (Madrid). 9/8/1864. Hemeroteca Digital BNE. https://hemerotecadigital.bne.es/hd/es/viewer?id=406c3c58-8b9c-4da4-8bf3-7ea2e709e2b3&page=3	21 ounces
Coll de Canas (Gerona)	6/7/1864	430	La Esperanza (Madrid). 1/8/1864. Hemeroteca Digital BNE. https://hemerotecadigital.bne.es/hd/es/viewer?id=3b344907-e950-497a-806a-28400a31ca20&page=3	15 ounces. Location approximate.
Beas de Segura (Jaén)	28/6/1863	460	La Correspondencia de España (Madrid). 5/7/1863. Biblioteca Virtual de Prensa Histórica. https://prensahistorica.mcu.es/es/catalogo_imagenes/grupo.do?path=6044358&posicion=2&presentacion=pagina	1 pound
Socuéllamos (Ciudad Real)	18/8/1862	690	Diario de Palma (Palma de Mallorca). 3/9/1862. Hemeroteca Digital BNE. https://hemerotecadigital.bne.es/hd/es/viewer?id=4f407890-4027-4dab-9c29-18e3caf181a6	24-ounces. Person dies afterwards due to injuries sustained from hailstones.
Hostalric (Gerona)	10/9/1861	920	El Contemporáneo (Madrid). 18/9/1861. Hemeroteca Digital BNE. https://hemerotecadigital.bne.es/hd/es/viewer?id=d9440efb-6ec2-4f3a-8710-65f760e8d305&page=4	More than two pounds.
Villareal (Castellón)	22/7/1860	460	La Época (Madrid). 26/7/1860. Hemeroteca Digital BNE. https://hemerotecadigital.bne.es/hd/es/viewer?id=44b4c38f-c8f0-41bd-b7e9-9fe39d597fec&page=4	Some more than 1 pound, most 2-3 ounces
Vinaroz (Castellón)	29/8/1859	920	El Estado (Madrid). 16/9/1859. Hemeroteca Digital BNE. https://hemerotecadigital.bne.es/hd/es/viewer?id=ae35740b-528d-4089-bfbb-2861280cf9e6	1-2 pounds.
Villavieja (Castellón)	26/8/1859	550	El Conciliador (Madrid). 2/9/1859. Hemeroteca Digital BNE. https://hemerotecadigital.bne.es/hd/es/viewer?id=285b63bf-6087-4a3e-8f33-be119ccaa9a9&page=3	Stone hit a roof, was picked up, and found to weigh 19 ounces.
Albacete (Albacete)	16/8/1859	1770	1) El Clamor público (Madrid). 19/8/1859. Hemeroteca Digital BNE. https://hemerotecadigital.bne.es/hd/es/viewer?id=0afe57a9-8001-4209-8253-f8e0e562348b&page=3 2) La Paz (Murcia). 20/8/1859. Biblioteca Virtual de Prensa Histórica. https://prensahistorica.mcu.es/es/catalogo_imagenes/grupo.do?path=1000100478&posicion=1&presentacion=pagina	A stone that entered a doorway during the storm was weighed in 4 pounds minus 2 ounces (1). Others collected after the storm weighed 20 ounces and 33 ounces. Other report (2) mentions 9-inch diameter hail and stones weighing 3 pounds and 2.5 ounces.
Caspe (Zaragoza)	21/7/1859	920	La Época (Madrid). 26/7/1859. Hemeroteca Digital BNE. https://hemerotecadigital.bne.es/hd/es/viewer?id=c4833d1a-79d1-4757-9ef7-b3161474043c&page=3	2 pounds.
Pego (Alicante)	5/8/1857	720	El Estado (Madrid). 24/8/1857. Hemeroteca Digital BNE. https://hemerotecadigital.bne.es/hd/es/viewer?id=57bd760e-f8fe-41f1-a324-846ae5bcdefc&page=3	25 ounces.
Ronda (Málaga)	8/8/1854	400	El Eco de Aragón (Zaragoza), p. 2. 22/7/1868. Hemeroteca del Ayuntamiento de Zaragoza. https://www.zaragoza.es/hemeroteca/prensa/HMZ_P0088/HMZ_P0088_1854-08-21/HMZ_P0088_1854-08-21.pdf	14 ounces
Guisona (Lérida)	27/7/1850	630	La Patria (Madrid). 3/8/1850. Hemeroteca Digital BNE. https://hemerotecadigital.bne.es/hd/es/viewer?id=296a6432-78cc-42a4-8938-d20b2542c37f&page=3	1.5 pounds. Torá and Guisona.
San Martí de Maldá (Lerida)	10/7/1850	460	El Bien público (Barcelona). 25/7/1850. Hemeroteca Digital BNE. https://hemerotecadigital.bne.es/hd/es/viewer?id=11f2a514-2060-4307-af8e-be6431c92ea2&page=2	1 pound